

Politecnico di Torino

Corso di Laurea Magistrale in
Ingegneria Energetica e Nucleare

Tesi di Laurea Magistrale
“Thermal analysis of laser ablation”



Relatori

Prof. Guido Perrone

Prof. Gianni Coppa

Candidato

Mirko Saccone

A.A. 2018/2019

Abstract

The heating up of the tumoral mass, aim of the procedure, must be made with particular care, considering the damage that could be caused to the healthy tissues surrounding the ablated area. The margin of tolerance around this area needs to be minimized. In order to achieve this result, the treatment planning must be as precise as possible: for this reason, a deep understanding of the process of shaping and of the physical parameters involved is needed. This work moves in this direction.

A parametrical analysis, by means of a software, has been performed to investigate the dependence of the ablated area geometry on the most important thermal parameters of this ablation technique.

During this preliminary phase doubts were raised over the only source of data available for the extinction factor in human liver. For this reason it was decided to verify experimentally the absorption-related data taken from the literature on which all of the simulations were based on, as of the start of this thesis, and to establish the behaviour of the same properties under thermal stress, simulating the ablation process.

Experimentally the procedure was the following:

- a comparison of the absorbance values from the literature with the measurements made in laboratory on bovine liver was performed;
- a measurement of the absorbance of the same samples, following a heating up to a temperature similar to the one typical of the ablation.

The results obtained showed a correspondence with the expectations but a sensible discrepancy with respect to the literature data. On the other hand, the samples subjected to heating increased their absorbance while maintaining a similar dependence with respect to the wavelength.

The results of this thesis are meant to shed some light on the role of the many parameters involved in this treatment and to investigate the promising possibility to tune them with a greater precision to minimize the quantity of healthy tissue damaged during the laser ablation.

Sommario

Il riscaldamento a fini terapeutici di una massa tumorale, scopo della procedura in esame, deve essere fatto con particolare, considerate il danno che potrebbe essere arrecato a tessuti sani intorno all'area da rimuovere. Il margine di tolleranza intorno a quest'area deve essere minimizzato e per ottenere questo risultato il piano terapeutico deve essere svolto con la massima precisione: per questa ragione una profonda conoscenza del processo di sagomatura dell'area riscaldata e di tutti i parametri che governano il processo è necessaria. Questo lavoro si muove in questa direzione.

Un'analisi parametrica, per mezzo di un software, è stata compiuta al fine di investigare la dipendenza delle dimensioni dell'area soggetta a riscaldamento rispetto ai più importanti parametri termici di questa procedura.

Durante la fase preliminare più di un dubbio è stato sollevato sull'attendibilità dell'unica fonte di dati disponibile per il coefficiente di estinzione nel fegato umano. Per questa ragione è stato deciso di verificare sperimentalmente i parametri legati all'assorbimento ottico su cui le simulazioni erano state basate fino a quel momento e di indagare il comportamento degli stessi parametri dopo aver sottoposto i tessuti ad un riscaldamento simile a quello tipico dell'ablazione laser.

Sperimentalmente la procedura è stata la seguente:

- una comparazione tra i valori della letteratura del coefficiente di estinzione e quelli ottenuti dalle misurazioni in laboratorio è stata effettuata;
- una misurazione dello stesso parametro, una volta sottoposto il campione a intenso riscaldamento, è stata poi condotta.

I risultati hanno mostrato una buona corrispondenza con le aspettative maturate nel corso dei diversi esperimenti svolti, anche prima di questa tesi. D'altra parte, i risultati ottenuti si scostano in maniera notevole rispetto ai dati presenti in letteratura.

Per quanto riguarda i campioni sottoposti a riscaldamento si è riscontrato un evidente aumento nell'assorbimento degli stessi, a fronte di un medesimo comportamento per quanto riguarda la dipendenza dalla lunghezza d'onda.

I risultati di questa tesi sono volti all'ottimizzazione dell'ablazione laser, nel tentativo di poter calibrare i parametri coinvolti in modo da minimizzare il danno ai tessuti sani.

Ringraziamenti

In questi tanti anni pregni di soddisfazioni, delusioni, euforia, stanchezza e di un'infinita curiosità, in questa costante fame di futuro, non ho probabilmente ringraziato abbastanza chi è stato il mio passato, è il mio presente e sarà il mio futuro: la mia famiglia. Grazie per aver capito, per esserci stati e per aver saputo non esserci, quando era l'unico modo per aiutare.

Grazie a Chiara, che mi ha conosciuto sprovveduto liceale e mi sta accompagnando nella scoperta del mondo. Senza di te avrei capito la metà delle cose.

Grazie ai miei amici, ai parenti e grazie a chi con un gesto ha tenuto viva in me, giorno dopo giorno, la speranza di un futuro radioso per me, per i miei cari e per tutti i passeggeri dell'astronave Terra.

Un ringraziamento al professor Perrone, relatore di questa tesi, la cui disponibilità è stata vitale durante l'intero periodo di stesura, e al professor Coppa, secondo relatore della tesi.

Ulteriori ringraziamenti al professor Vallan e a Massimo Olivero per la preparazione e l'esecuzione della parte sperimentale e a Jennifer Pogliano, per aver pazientemente condiviso le sue conoscenze nell'ambito dell'analisi computazionale.

Table of contents

Introduction.....	6
Thermal therapies.....	6
Hyperthermia	7
Ablation	10
Radiofrequency	10
Microwave	11
High intensity frequency ultrasound.....	12
Choice of the treatment.....	13
Laser ablation.....	14
Equipment.....	15
Source	15
Optical fiber	17
Prospective.....	18
Treatment planning	19
Monitoring	20
Future market.....	22
Thermal considerations.....	23
The Pennes' bioheat equation	23
Simulations	26
COMSOL.....	26
Model developed.....	28
Assumptions.....	28
Geometry.....	28
Boundary conditions	29
Mesh.....	29

Mesh refinement	30
Grid independence	30
Time-step independence	32
Parametrical analysis	33
Choice of the parameters.....	35
Results.....	36
Dependence on treatment time.....	36
Dependence by the thermal conductivity.....	38
Dependence by the laser power	39
Experiments	41
Experimental equipment	41
Source	41
Transmission.....	43
Optical Spectrum Analyser.....	46
Execution	46
Results.....	47
Considerations and further assumptions	47
Data	48
Conclusions.....	53
References.....	54

Introduction

Cancer is the second cause of death, globally, and made approximately 8.93 million victims in 2018. [1] This means that about one death out of six has been due to cancer. This statistic alone should give an idea of how important the world-wide fight against cancer is, daily carried on by thousands of researchers.

Cancer, however, is a broad term: it describes the disease that results when cellular changes cause the uncontrolled growth and division of cells. Some types of cancer cause rapid cell growth, others cause cells to grow and divide at a slower rate or interdict the apoptosis, the natural death of the cell. The result is lack of oxygen and nutrients that would usually nourish other cells. In general, this process can determine visible growths, called tumours, or involve different mechanisms, as it happens with leukaemia.

The importance of finding a solution to the several forms of cancers goes hand in hand with the difficulty of treating the huge variety of them. The National Cancer Institute, counts more than 100 different type of cancers, even neglecting the peculiarities of each clinical record. [2] Indeed, cancer has not only a way to manifest itself and, because of this, very different strategies have to be adopted to treat every patient. The most adopted treatments are chemotherapy, radiotherapy and surgery, often combined among them. Anyway a certain number of alternative treatments can be a viable choice, now and in the future. Among the latter thermal therapies have been recognized to be a reasonable option in many different clinical situations, thanks to the technological and scientific progresses recently made in the field.

Thermal therapies

The use of thermal energy for therapeutic purposes dates back thousands of years.

It is well-known that thermal baths were common among the wealthy citizens of the Roman Empire but not so many knows that often complete facilities for the treatment of diseases were present in thermal baths. The oldest report is dated 3000 BC and was found on an Egyptian papyrus concerning surgical procedures. [3]

Thermal therapies include all the medical applications which use a heat source to increase the temperature of some part of the human body for a certain quantity of time. This very generic definition leave room for interpretation: is the heat source internal or external? What temperature do I want to obtain and where? On a local spot or all over a broad part of the body? For how long? Answering these question helps us navigating from the self-care treatment for arthritis to the laser tumour ablation: even if both could be referred to as thermal therapy they are poles apart.

The first distinction that can be made for thermal therapies is between hyperthermia where temperature is raised above the normal body level and hypothermia, where on the contrary, temperature is decreased. While some interest has been raised also for hypothermia, the main branch is hyperthermia when dealing with cancer.

Cancer cells, similarly to any other cell and living system, respond to mild changes of external temperature by activating homeostatic biological mechanisms, in an attempt to sustain a tolerant intracellular environment and prevent death. However, temperatures above 41°C are toxic both to the tumour vasculature and to the cancer cells themselves and are used to suppress tumour growth, achieve regression or to sensitize them to radiotherapy and chemotherapy. [4]

Hyperthermia

Hyperthermia can be categorized according to the temperature reached during the treatment:

- Low temperature hyperthermia, also called diathermia, reach temperatures around 41°C and brings a general increase of the metabolism resulting in an accelerated tissue repair;
- Moderate temperature hyperthermia, with temperature below 45°C, is generally used to increase cell sensitivity to the primary therapy;
- High temperature hyperthermia, also called ablation, using temperature above 50°C aims to denaturize proteins inside the cells and bring to the death of them. [3]

Naturally different approaches and different temperature fields will determine different damage to the tumoral and surrounding tissue. To evaluate the thermal damage and cell death processes the Arrhenius law has been used for decades with good results. [5]

Its formulation is:

$$\Omega = \int_0^{\tau} A \cdot \exp\left(\frac{E_a}{R \cdot T}\right) dt$$

where

- Ω is the relative damage to the tissue;
- A is frequency factor;
- E_a is the activation energy;
- R is the universal gas constant;
- T is the absolute temperature;
- τ is the total exposure time.

The tissue is assumed to be irreversible damaged when $\Omega = 1$ which is corresponding to a denaturation of 63% of the molecules.

Nevertheless, from an experimental point of view, what is more relevant is to be able to compare different treatments in terms of time and temperature achieved: for this reason, a standardized equivalent value has been defined, the cumulative equivalent minutes at 43°C, CEM43°C

$$CEM43^{\circ}C = t \cdot R^{(43-T)}$$

where

- t is the time interval in minutes;
- R is a coefficient equal to 0.5 for temperature higher than 43°C and to 0.25 for temperatures lower than 43°C;
- T is the temperature in Celsius.

Figure 1 and 2 show some explicative plots.

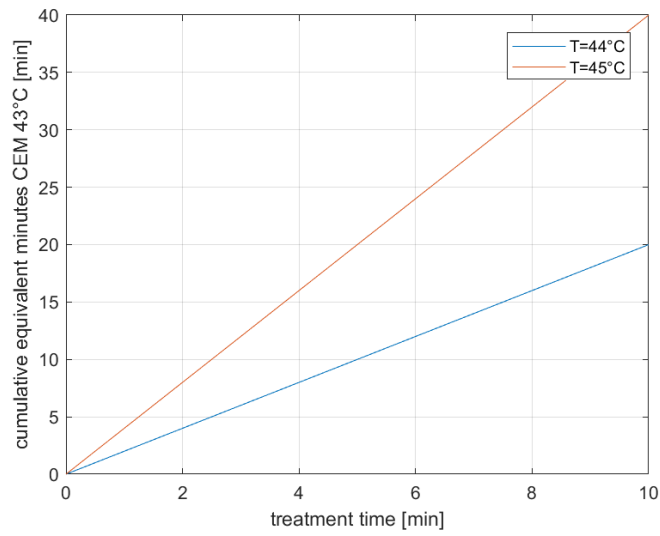


Figure 1

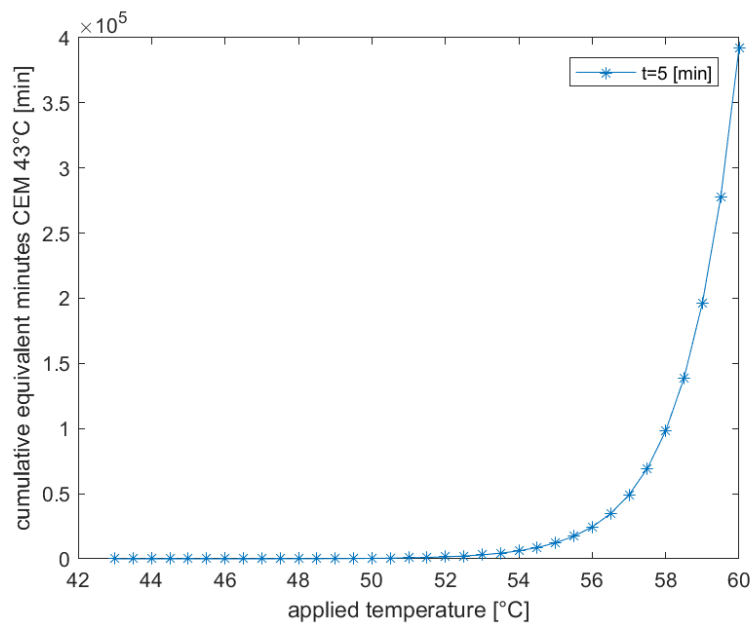


Figure 2

This comparison method is called “thermal isoeffective dose”. [6]

If greater precision is to be achieved, however, rate of the temperature increase and induced thermo-tolerance should be considered, tuning the thermal dose accordingly.

Ablation

Aiming to temperatures above 50°C ablation is performed locally with great care on minimizing the healthy tissue involved. In order to do so, needle-like probes are generally inserted in the tissue percutaneously or laparoscopically: tumour ablation is indeed a minimally invasive technique or even non-invasive, if ultrasound are adopted. Due to these features, thermal ablation is characterised by quicker recoveries and fewer complications compared to surgical resection. [7]

Among the possible ablation techniques there are some used worldwide: radiofrequency (RF), microwave (MW), laser (LA), high intensity focused ultrasound (HIFU). As of today radiofrequency ablation is the most used one, dominating the market of ablation, and microwave ablation is trying to keep the pace. However, each modality has optimal working conditions which make it suitable for different tumours. As may be expected, choosing the most appropriate technique is crucial to the success of the intervention.

Radiofrequency

Radiofrequency ablation creates a circuit within the body of the patient using an oscillating current to produce Joule heating. A needle-like electrode is inserted in the proper position to ablate the tumour. The circuit is completed by a dispersive electrode typically placed on the skin of the patient in a monopolar configuration or by a second needle-like electrode if bipolar RF ablation is used. Most currently available RF systems operate with monopolar electrodes mainly to reduce the invasiveness of the procedure.

Alternating current is used (rather than direct) to avoid stimulating nerve cells and causing pain. When AC is

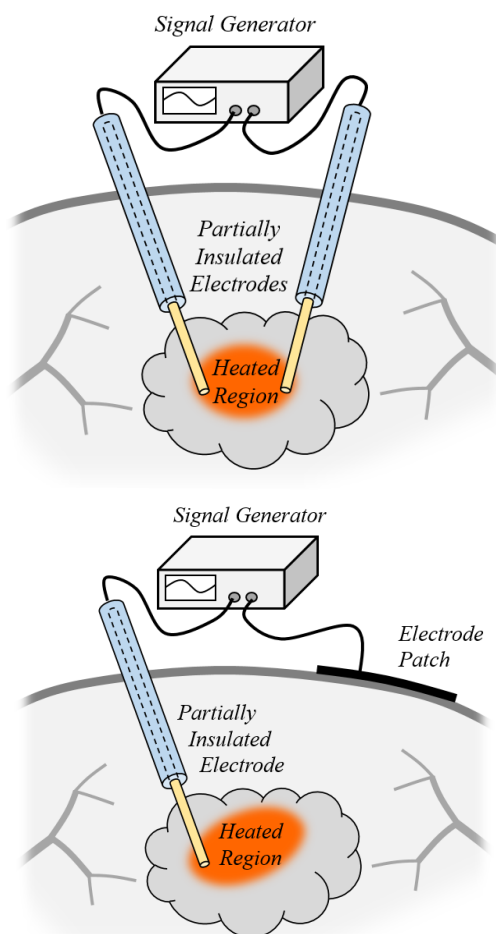


Figure 3, from [8]

used, and the frequency is high enough (300 to 500 kHz), the nerve cells are not directly stimulated. [8]

Tissues are in general poor electrical conductors so the current will be easily increased. In particular, closest to the electrodes the tissues are subject to resistive

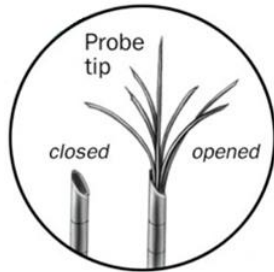


Figure 4, from [9]

heating while further away thermal conduction plays a major role. This is the reason why, in the most used configuration, the probe tip has been designed to come out of the catheter, when already in position, and spread its extremities as shown in the figure in order to widen the area subject directly to Joule heating. Even so, some applicators still use a single tip. This can be reasonable in some clinical conditions.

Radiofrequency ablation, furthermore, is what is commonly called a self-limiting process: the ablated tissue loses its electrical conductivity and makes the process more and more difficult, while it is carried out. This is the main drawback of this ablation approach.

Microwave

In this procedure, microwaves transmitted through the probe are used to heat and destroy the abnormal tissue. [10] When electromagnetic energy is applied to a tissue, polar molecules, such as water, continuously attempt to align with the oscillating electromagnetic field. The inability of such molecules to keep up with the rapidly oscillating field leads to energy absorption and tissue heating. Thus, tissues that have high water content (for example liver and kidney) are heated most readily during MW ablation. This makes MW ablation useful in tissues with poor electrical conductance, such bone, lung, and ablated tissue. Additionally, because MW fields can overlap in tissue, multiple applicators can be used simultaneously to create larger

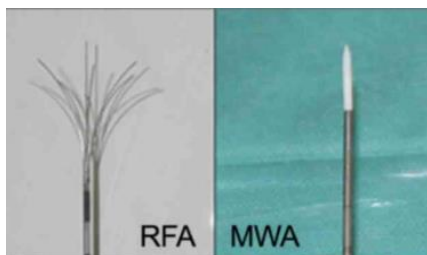


Figure 5, from [11]

ablations once it has been clinically considered the increase of the invasiveness. As the Figure 5 shows, anyway, the tip of the applicator in this case is generally different from the one used in RF ablation. Indeed MW ablation the single tip is the only viable option.

One of the drawbacks of microwave ablation is the need for a cooled shaft, in certain cases. This, naturally, makes the set-up more expensive.

High intensity frequency ultrasound

HIFU is the only non-invasive method among the one analysed in this work: it exploits the ultrasound waves, the same used for diagnostic purpose although with increased intensity.

Each beam is precisely focused on a small region of diseased tissue to locally deposit high levels of energy. The temperature of tissue at the focus will rise to between 65 and 85 °C, destroying the diseased tissue by coagulative necrosis. [12]

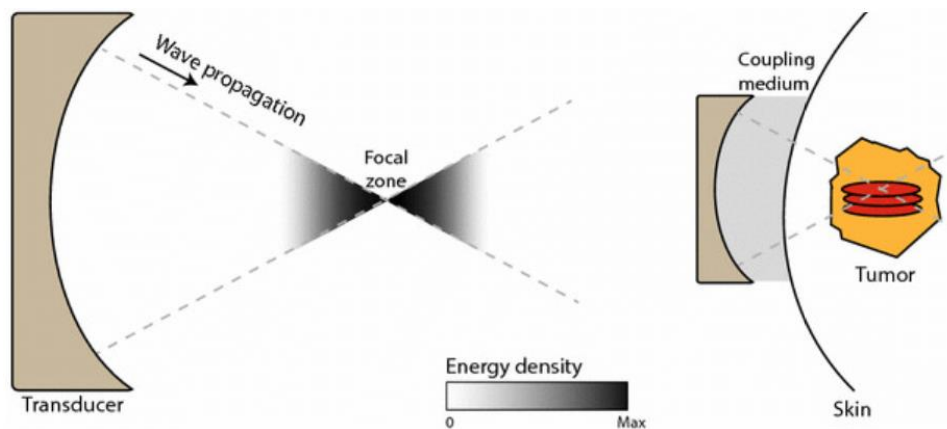


Figure 6, from [13]

Even if the damage to cells is primarily thermal HIFU treatments lead to a non-negligible mechanical stress in the tissue: the formation of cavitations and their fast change in size ends in a collapse that releases shock waves into the surrounding tissues causing mechanical damage.

The cytotoxic heating and mechanical effects on the targeted tissues can be performed through intact skin or mucosa. This makes HIFU a very attractive option for many cancers. However, non-invasive treatment with HIFU does have several limitations. The lesions treated most effectively by HIFU are mostly superficial owing to limitations in ultrasound penetrance through many tissues. Additionally, the high-intensity ultrasound waves are subject to scatter and reflection, which can

lead to injury of tissues adjacent to the targeted area, such as skin burns, damage to peripheral nerves, or bowel injury. [14]

Choice of the treatment

The choice of the treatment to be used is, as already said, fundamental. In this decision two parameters have a crucial importance: the type of tissue to be ablated and the size of the area.

Generally, RF and LA ablation are usually preferred to MW for the treatment of nodule with diameter smaller than 2 centimetres, since they are cheaper than the latter, but if the tissue is strongly perfused MW ablation should be considered. If the treatment is carried out on a high-risk location LA is, in most cases, favoured.

MW ablation may be applicable to a broader spectrum of tissues. It is less sensitive to perfusion and it can cover a larger area. Furthermore, newer generation MW systems may even be more effective for larger tumours, but longer-term clinical data are needed to evaluate the role of tumour size on MW ablation efficacy. [14]

Laser ablation

Laser ablation is becoming a valid alternative to surgical resection. The heat deposition in this type of ablation is obtained by the scattering and the absorption of the light energy emitted by the laser. The devices and systems used for laser tumour ablation are similar to those used for other clinical laser treatments.

At the time this thesis is written, the most employed configuration uses light generated by neodymium-doped yttrium aluminium garnet lasers (wavelength of 1064 nm) applied to the target tissue using a fiber optic applicator. Infrared energy penetrates tissue directly for a distance of 12-15 mm, although heat is conducted beyond this range creating a larger ablative zone. Furthermore, optical penetration has been shown to be increased in malignant tissue compared to normal body mass.

Temperatures above 55-60°C cause rapid coagulative necrosis and instant cell death, but irreversible cell death can also be achieved at lower hyperthermic temperatures (> 42°C) although longer durations are required, as already mentioned in the previous sections. Temperatures above 100°C will cause vaporisation from evaporation of tissue water and above 300°C tissue carbonisation occurs. Overheating is thus best avoided as carbonization decreases optical penetration and heat conduction and limits the size of lesion produced. Local tissue properties, in particular perfusion, have a significant impact on the size of ablative zone. Highly perfused tissue and large vessels act as a heat sink. [16]

There are several methods exploited to manipulate the volume ablated: for example, applicators with a scattering or diffusing tip are often used to increase mentioned volume. The simplest methods, anyway, are the customization of the fiber and the combined use of sources at different wavelengths. Jennifer Pogliano, while working to her thesis at the Electronics and Telecommunications Departments (DET) of the Polytechnic of Turin, made some experiments on the customization of the fiber, showing how the delivered power can be spread over a larger volume if the fiber is modified accordingly. [17]

Another alternative solution for the shaping which is noteworthy are the use of nanoparticles in the photothermal ablation of cancer. The basis of this therapy is that materials that highly absorb light can be designed and delivered specifically to the

tumour cells. The subsequent application of light will then cause specific thermal killing to nanoparticle tagged tumor cells.

Gold based nanoparticles have been designed and absorb light in the near-infrared (NIR) region where water and hemoglobin show high transmissivity. If the nanoparticles are selectively accumulated in the tumor, the light will be mostly absorbed by the tumour only. As a consequence, the absorbed light that is converted into heat energy causes a temperature increase localized in the target. This specificity depends on the geometry, morphology, and surface charge of the nanoparticles; therefore, several kinds of gold nanoparticles have been designed for photothermal ablation to optimize the absorption and selectivity.

Clearly, the use of nanoparticles in this treatment approach is in its infancy. The early promising results bring expectations that this approach may have an important future clinical impact. Further improvements and successful introduction in therapy require a proper evaluation and understanding of their interactions with biological entities and their potential for inadvertent toxicities. [18]

Equipment

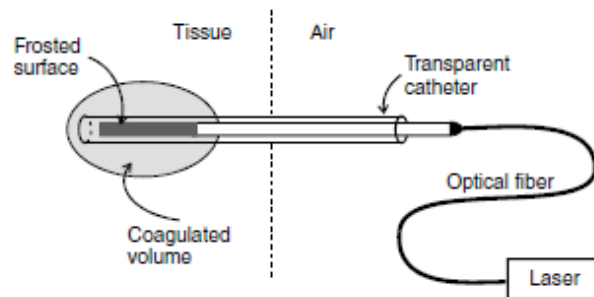


Figure 7, from [19]

The equipment needed during the ablation is clumsily depicted here: the laser source, the transmitting fiber and the ending part of the fiber, enveloped in a transparent semi-rigid catheter to simplify the positioning inside the body. The source and the optical fiber are the technological spine of the whole process so they deserve a detailed insight.

Source

The source employed in this ablation process is a laser, from which it takes the name.

Laser technology is at the core of the wider area of photonics, essentially because laser light has a number of very special properties:

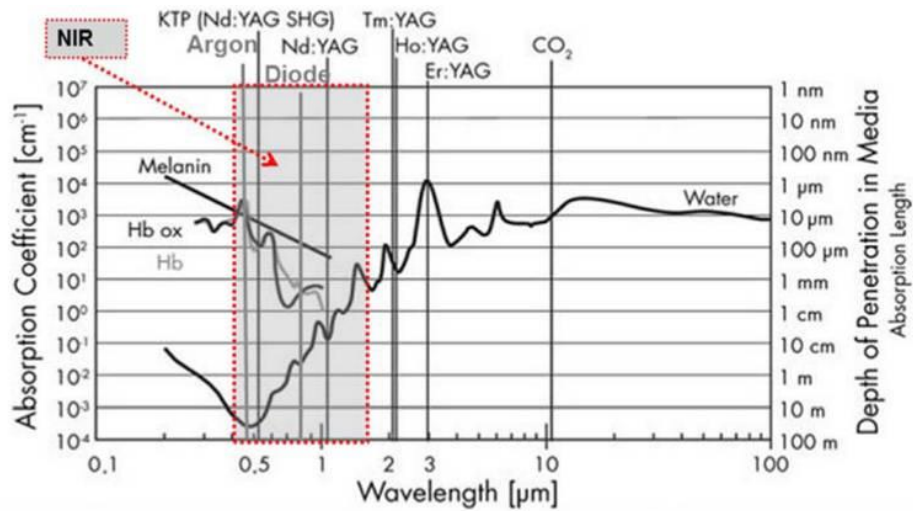
- It is usually emitted as a laser beam which can propagate over long lengths without much divergence and can be focused to very small spots.
- It can have a very narrow optical bandwidth, whereas e.g. most lamps emit light with a very broad optical spectrum.
- It may be emitted continuously, or alternatively in the form of short or ultrashort pulses, with durations from microseconds down to a few femtoseconds.

These properties, which make laser light very interesting for a range of applications, are to a large extent the consequences of the very high degree of coherence of laser radiation.

Common types of lasers are:

- Semiconductor laser diodes, as Ga-As and InP alloys;
- Solid-state lasers based on ion-doped crystals. Common gain media are Nd:YAG, Nd:glass, Yb:YAG;
- Fiber lasers, based on optical glass fibers, especially the rare earth-doped fibers, for example the Yb-doped ones;
- Gas lasers, as the CO₂ lasers. [9]

In the laser ablation applications many different types of laser have been proposed in the last years in order to obtain different temperature fields: the effects of laser light on tissue depend on their wavelength, hence absorption length. We can see an explicative plot in Figure 8.



Laser	Wavelength [nm]	Penetration depth [cm]	Mode
Nd:YAG	1064	≈1–10	Pulsed/continuous
diode	800–980	≈1–50	Pulsed/continuous
Ho:YAG	2100	≈0.04	Pulsed
KTP	532	>1000	Quasi continuous
Tm:YAG	2016	≈0.01–1	Continuous

Figure 8, from [17]

Even if the Nd:YAG laser is the main choice nowadays, the possibility of using different sources is a non-negligible degree of freedom for future applications.

Optical fiber

The light emitted by the source is guided to the ablation area by mean of an optical fiber. Optical fiber has been an enabling technology for laser-based medical applications: these have increased and become more attractive with the development of optical fibers allowing access to biological tissue.

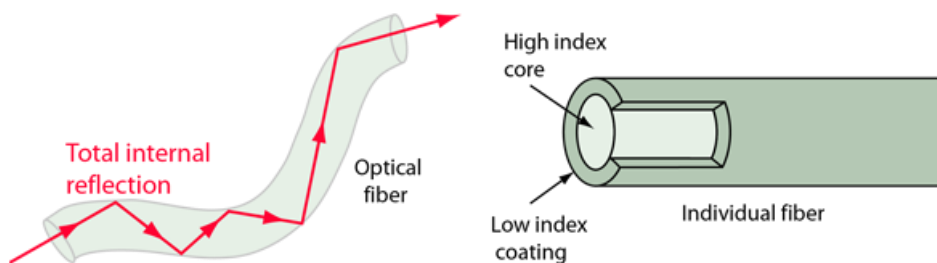


Figure 9, from [9]

These systems changed the world of long-distance communication because of an optical phenomenon that allows them to act as waveguides with minor losses: the total internal reflection, often referred to using the acronym TIR. [20]

This phenomenon is controlled by the angle of incidence between the wave and the medium-to-medium interface crossed.

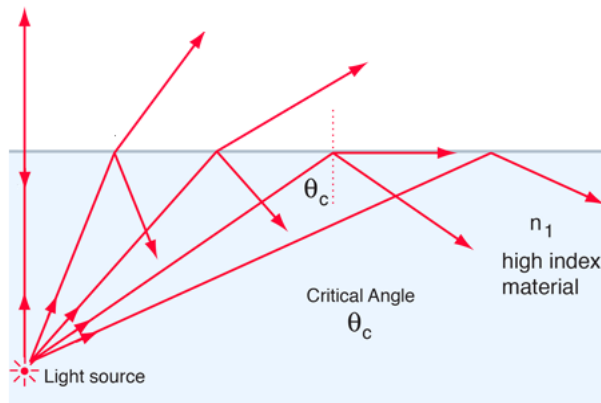


Figure 10, from [21]

Light striking a medium with a lower index of refraction (with respect to the medium it was travelling in) can be totally reflected. In particular if the angle of incidence is higher than a critical value θ_c , light is totally reflected.

Prospective

After the tumour localization and the identification of its features (geometry, contours, histology), there are two main challenges in LA: an accurate placement of the applicator in the tumour, and accurate treatment planning and monitoring. New Hyperthermal Treatment Planning (HTP) tools and monitoring tools are beginning to overcome some of these challenges, and they are gaining widespread attention and broad clinical acceptance as techniques for improving the safety and outcomes of thermal treatments.

It is commonly accepted, among researchers working in this field, that achieving a high accuracy in controlling the amount of heat delivered on damaged tissues and on the surrounding area is fundamental in terms of clinical impact. For this reason much effort has been recently put in this direction and not only: the improvement of new solutions for real time thermometry, and to the use of tumor targeted nanoparticles are also very interesting topics for researchers, as of now. In this section, the basis and the most significant challenges of these three promising solutions will be described.

Treatment planning

HTP aim at establishing the treatment settings that maximize the thermal treatment quality. HTPs model the interaction between the energy delivered by the thermal treatment and the tissue, in order to obtain a prediction of the tissue temperature distribution and therefore the amount of damaged tissue volume.

Generally, the simulations can be divided in three steps:

- the first step is the generation of the patient model, aimed at obtaining a description of the geometry and of the physical properties of the tissue undergoing the treatment. This first step is crucial because the geometry and characteristics of the tissue strongly influence the interaction between the tissue and the energy delivered to treat the tumour;
- the second step is focused on the calculation of the amount of power absorbed by the tissue. Obviously the models employed depend on the kind of device used to induce the hyperthermia. In LA, the simulation is aimed at calculating the light distribution within the tissue. This task is usually performed using the Monte Carlo simulation and requires the knowledge of the tissue optical properties at the used laser wavelength and the emission modality of the applicator;
- the third step provides the tissue temperature distribution. The model most widely used to perform this prediction is the Pennes' equation, that will be analysed in one of the following sections. The accurate prediction of temperature can determine a step change in the treatment outcomes. [17]

The importance of HTP tools in current clinical settings is confirmed by the recent decision of the European Society for Hyperthermic Oncology to include HTP in their quality assurance guidelines for deep hyperthermia [22], and by the recent development of several commercial treatment planning. HTP tools go through a severe evaluation and validation. Recently, Hyperplan, one of the tools developed ad hoc for ablation, predicted both the occurrence of discomfort and its location in a cohort of 30 patients with an error of the temperature prediction lower than 4 °C. HTP tools have been also used for improving the safety and effectiveness of local hyperthermal treatments combined with radiotherapy and chemotherapy. Despite the HTPs limitations in the accurate prediction of the temperature distribution, they have demonstrated marked improvements over the last few years, so their integration into the clinical workflow is gaining acceptance. In addition, temperature feedback

obtained by thermometric techniques could correct HTP prediction during the treatment.

Monitoring

The importance of temperature monitoring during LA can be motivated by considering that the amount of damaged tissue depends on both the tissue temperature map and the exposure time; for this reason the knowledge in real time of the tissue temperature may be particularly beneficial for the optimization of laser settings applied during treatment. Thermometric techniques can be divided in two categories: invasive techniques and non-invasive techniques. [17]

Among the invasive thermometric techniques, the most largely employed transducers are thermistors, thermocouples, and fiber optic-based sensors. Their use has been investigated in many recent in vivo and ex vivo cancer thermal treatment studies and on different organs. They allow for real time temperature monitoring with good spatial resolution, and quite good (thermocouples) or good (thermistors) accuracy. Their main drawbacks are related to their intrinsic invasiveness, and measurement only at a single point. There can also be measurement errors due to the strong light absorption of the wires of the thermocouple and due to the high heat conduction for both thermocouples and thermistors.

Among the fiber optic-based sensors the most relevant are the Fiber Bragg Grating (FBG) sensors.

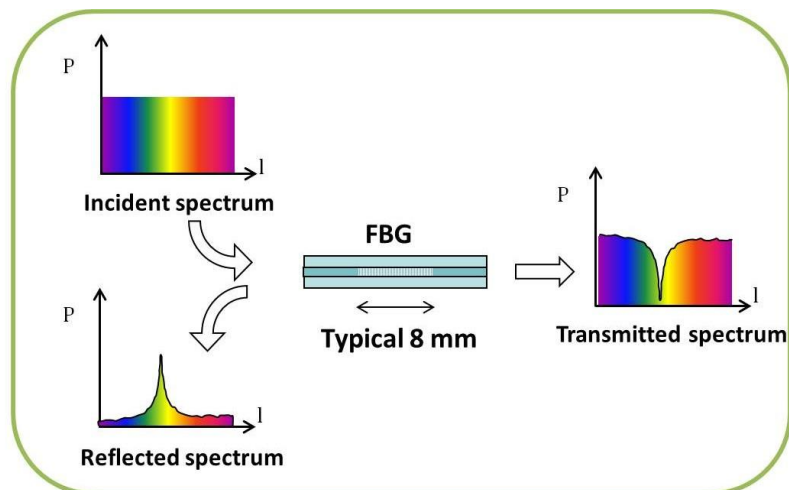


Figure 11, from [23]

Fiber Bragg Gratings are made by laterally exposing the core of a single-mode fiber to a periodic pattern of intense ultraviolet light. The exposure produces a permanent increase in the refractive index of the fiber core, creating a fixed index modulation according to the exposure pattern. This fixed index modulation is called a grating.

The reflection wavelength of the FBG, namely the Bragg wavelength, depends on the grating characteristics and is influenced by the ambient conditions such as strain and temperature. This allows the utilizations of FBGs as sensor for strain and temperature: it is obvious that, when using them as a temperature sensor, the dependency on the strain is a parasitic effect that substantially hinders my measure producing measurement errors during in vivo trials caused by the respiratory movements of the patients. Temperature probes embedding FBGs within a needle have been proposed to tackle this problem. [24][25]

These sensors have been introduced in this field more recently than thermocouples and thermistor. Their main advantages are related to due to their immunity from electromagnetic fields and their MR-compatibility, which allows for using this sensor during MR-guided procedures. Their small size and flexibility, short response time, good spatial resolution, and good accuracy (≈ 0.2 °C) are also assets. Their main drawbacks are related to their invasiveness and to the strains applied that hamper the measurements. [25]

The most promising non-invasive thermometric methods are MR-based thermometry and CT (Computed Tomography)-based thermometry.

Basically, MR-thermometry is founded on the dependence of a number of MR parameters on temperature. After the reference in term of temperature dependence of the parameter has been taken with some experiments this technique allows to obtain a good spatial and temporal resolution. MR thermometry has been used extensively in LA for HCC. [17]

CT-thermometry was first investigated during the 1970s, but investigations were discouraged by the limitation of the CT scan in terms of reproducibility and stability. In the last decade, the improvements of CT scanners have encouraged a number of groups to use this method in thermal treatment. During the last few years this technique has been mainly employed during ex vivo experiments and on phantoms. [26] Although laser ablation guided by non-invasive thermometry is in its infancy,

recent technical solutions are helping to increase the number of studies in animal models and in humans.

The main advantages of these two non-invasive techniques are related to the non-invasiveness and to the possibility of obtaining a three-dimensional temperature distribution. The main disadvantages of MR-thermometry are related to the cost of the MR scan, cost of custom-made sequences to obtain good thermal sensitivity, and the hazards of working in an MR environment; the main drawback of the CT-based thermometry is related to the use of ionizing radiation.

Future market

A report by Grand View Research states that the global tumor ablation market size is foreseen to reach USD 2.17 billion by 2025. This would be a huge result. Anyway this forecast stands on solid basis: increasing cases of cancer across the globe is the key growth-driving factor for this market. About 13.0% of the population suffers from cancer each year, as per the statistics by the World Health Organization (WHO) mentioned in the first section.

Demand for minimally invasive procedures due to the benefits, such as less trauma, speedy recovery, along with technological advancements in the field of thermal ablation is also likely to boost market growth.

Increasing per capita income is enabling people to take up advanced treatment for tumours, thus driving the growth of this market. Active role of healthcare agencies and government in creating awareness about various cancer types is also expected to facilitate usage of tumour ablation therapy, thereby supporting market development.

[27]

Thermal considerations

The temperature field in the tissue, is determined by the heat deposition of the light energy and, indirectly, by heat conduction. Although the conduction is only a secondary phenomenon it is often referred as the main actor in the equation regulating the process, while the heat deposition is usually confined in a source

In 1948, Pennes performed a series of experiments that measured temperatures on human forearms of volunteers and derived a thermal energy conservation equation. From that moment on the Pennes' bioheat transfer equation (PBHTE) has been a standard model for predicting temperature distributions in living tissues. The equation has its main difference with respect to the general heat conservation equation in the special term that describes the heat exchange between blood flow and solid tissues.

The Pennes' bioheat equation

$$\rho \frac{\partial T(\vec{r}, t)}{\partial t} = \nabla \cdot (k(\nabla T(\vec{r}, t))) + Q_{laser}(\vec{r}, t) + \rho_b \omega_b c_b (T(\vec{r}, t) - T_b) + Q_m(\vec{r}, t)$$

where

- ρ is the density of the tissue and ρ_b is the blood density $\left(\frac{\text{kg}}{\text{m}^3}\right)$;

- k is the tissue thermal conductivity;

- Q_{laser} is the volumetric power deposited by the laser $\left(\frac{\text{W}}{\text{m}^3}\right)$;

- ω_b is the perfusion rate $\left(\frac{1}{s}\right)$;

- c_b is the specific heat of the tissue $\left(\frac{J}{\text{kg}\cdot K}\right)$;

- Q_m is the volumetric metabolic heat generation $\left(\frac{\text{W}}{\text{m}^3}\right)$.

If the assumptions listed in the section "Model developed" are considered the perfusion and the metabolic heat generation are neglected and the equation gets easier:

$$\rho \frac{\partial T(\vec{r}, t)}{\partial t} = \nabla \cdot (k(\nabla T(\vec{r}, t))) + Q_{laser}(\vec{r}, t)$$

That is a simple transient heat conduction problem in presence of a source if the light energy deposition problem is assumed to be solved independently. This is an assumption close to reality as the optical parameters have a weak temperature dependence.¹⁶

Normally the blood temperature is assumed to be constant arterial blood temperature.

Concerning $Q_{laser}(\vec{r}, t)$ it has to be reminded that the energy emitted from the fiber tip is absorbed by the tissue according to the Beer- Lambert law

$$I(x) = I_0 \cdot e^{-\alpha x}$$

giving the source a decreasing exponential shape. This, as mentioned in the laser section of this thesis, brings the intensity of the beam to decrease very rapidly and fall to the 13% of the initial value by covering one penetration depth δ .

$$\delta = \frac{1}{\alpha}$$

The attenuation constant for an electromagnetic wave at normal incidence on a material is also proportional to the imaginary part of the material's refractive index n . Using the above definition of α (based on intensity) the following relationship holds:

$$\alpha = \frac{2\omega}{c} \cdot \text{Im}(n) = \frac{4\pi}{\lambda} \cdot \text{Im}(n)$$

where

- $\text{Im}(n)$ denotes the complex index of refraction;
- ω is the radian frequency of the radiation $\left(\frac{1}{s}\right)$;
- c is the speed of light in vacuum $\left(\frac{m}{s}\right)$;
- λ is the related wavelength (m).

This is a key concept in this thesis: the only available data source for human liver absorption is, as of now, the work of Giannios et al. [28], which determines the

values of the imaginary part of the refractive index, as a function of the wavelength. For this reason, this physical relationship has been widely used during the experimental part of this thesis.

Simulations

The solution of the computational problem is the only way to obtain the temperature field described by the Pennes' equation without applying strong assumptions that are usually far from the reality.

The improvement in the precision and the decrease of the computational cost of these simulations could determine a step-change in the field. It has to be reminded that precise and verified simulations are not only necessary for a reliable treatment planning aiming to minimize the healthy tissue involved but have crucial implications in the control of the process during the ablation itself.

In this thesis a computational tool has been used to perform simulations of a simple model describing human liver undergoing laser ablation. In particular COMSOL (version 5.2a) has been used.

COMSOL

COMSOL is a platform that allows the numerical solution of partial differential equations. In particular COMSOL uses a "Multiphysics" approach allowing to couple related physical applications together and, for this reason, to include all the necessary factors for a complete model. Hence it can be said that COMSOL Multiphysics is a simulation software designed to minimize the assumptions its users must make.

The different physics implemented are contained inside "modules" and in the version used 26 of them are available for use. For the development of the model employed in this thesis the Heat transfer module and the Ray optics module have been used.

The Heat Transfer module takes into account all the heat transfer modes:

- conduction, that occurs as a consequence of different mechanisms in different media. Theoretically, it takes place in a gas through collisions of molecules; in a fluid through oscillations of each molecule in a "cage" formed by its nearest neighbours; in metals mainly by electrons carrying heat and in other solids by molecular motion, which in crystals take the form of lattice vibrations known as phonons. In a continuous medium, Fourier's law of heat conduction states that the conductive heat flux, q , is proportional to the temperature gradient. The coefficient of proportionality, k , is the

thermal conductivity and takes a positive value meaning that heat flows from regions of high temperature to low temperature;

- convection, a phenomenon that takes place through the net displacement of a fluid that transports the heat content with its velocity; the term convection often refers to the heat dissipation from a solid surface to a fluid, typically described by a heat transfer coefficient.
- Radiation, Heat transfer by radiation takes place through the transport of photons. Participating media absorb, emit, and scatter photons. Opaque surfaces absorb or reflect them.

Specifically in solids, COMSOL solves the following equation:

$$\rho \cdot c_p \left(\frac{dT}{dt} + u_{trans} \cdot \nabla T \right) + \nabla \cdot (q + q_r) = \alpha T : \frac{dS}{dt} + Q$$

where

- ρ is the density $\left(\frac{kg}{m^3}\right)$;
- c_p is the specific heat capacity at constant stress $\left(\frac{J}{kg \cdot K}\right)$;
- u_{trans} is the velocity vector of translational motion $\left(\frac{m}{s}\right)$;
- q is the heat flux by conduction $\left(\frac{W}{m^2}\right)$;
- q_r is the heat flux by radiation $\left(\frac{W}{m^2}\right)$;
- α is the coefficient for thermal expansion $\left(\frac{1}{K}\right)$;
- S is the Piola-Kirchoff stress tensor (Pa);
- Q is an additional heat source $\left(\frac{W}{m^3}\right)$.

The first term on the right-hand side is the thermoelastic damping. It has to be reminded that the d/dt operator represents the material derivative.

For what concerns the other module used in these simulations, the Ray Optics module, it allows, through the Geometrical Optics Interface, to compute the trajectories of the rays release by the laser. This module has been chosen over the Wave Optics module since it allows a simplification of the model and a lower

computational load, if the sizes of the geometrical entities, in the domain, are much larger than the wavelengths considered. In the employed module, for each ray, a set of coupled differential equations is solved to determine the components of the ray position and the wave vector. [29]

Model developed

Assumptions

The most important assumptions made for this model are:

- homogeneous properties, since the properties are not considered dependent on the spatial variable;
- isotropy of the material;
- negligible evolution in time of the properties;
- negligible metabolic heat generation;
- absence of close large vessels and negligible contribution of perfusion.

Geometry

The geometry used for the simulations is here presented: putting the source at the origin of the reference frame the tissue has been modelled as a simple sphere with radius large enough to allow the definition of the constant human body temperature at the interface. Specifically, the radius has been chosen to be 5 cm.

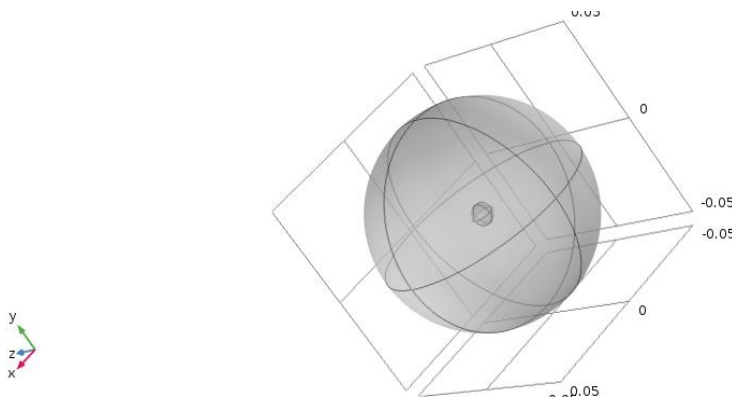


Figure 12

In the Figure 12 a smaller sphere can be seen: it is an artificial domain created for meshing purposes and has not physical meaning. Please refer to the *Mesh refinement* section for further explanation.

The choice of the 3D modelling over the simpler 2D approach has been made to allow the customization of the model for further, more complex, set-ups and the comparison with the reference situation developed here.

Boundary conditions

The boundary conditions were set to be of the Dirichlet type: fixed temperature, 37°C. Given the distance of the boundary from the point of heat deposition, indeed, it is reasonable to assume a negligible variation of the temperature from the body initial condition.

Moreover, all thermoregulation mechanisms of the human body are designed to return your body to homeostasis. This is a state of equilibrium, naturally. If we assume that the patient is not being put under physically stressful conditions this assumption an accurate reflection of reality.

Mesh

Tetrahedral elements are the default element type for most physics within COMSOL Multiphysics. Tetrahedra are also known as a simplex, which simply means that any 3D volume, regardless of shape or topology, can be meshed with tetrahedral elements. They are also the only kind of elements that can be used with adaptive mesh refinement. For these reasons, tetrahedral mesh can usually be your first choice.

The other three element types (bricks, prisms, and pyramids) should be used only when it is motivated to do so. It is first worth noting that these elements will not always be able to mesh a particular geometry. Furthermore the software requires a significative number of settings as input for the building meshes made of prisms and pyramids and the amount of work request usually tends to make tetrahedral elements the most common choice, if it is not needed to have a different approach. The pyramids are only used when creating a transition in the mesh between bricks and tetrahedral elements.

The primary motivation in COMSOL Multiphysics for using brick and prism elements is that they can significantly reduce the number of elements in the mesh. These elements can have very high aspect ratios (the ratio of longest to shortest edge), whereas the algorithm used to create a tetrahedral mesh will try to keep the aspect ratio close to unity. It is reasonable to use high aspect ratio brick and prism

elements when you know that the solution varies gradually in certain directions or if you are not very interested in accurate results in those regions because you already know the interesting results are elsewhere in the model. [30] However a similar result can be obtained meshing the different regions with a different resolution: the latter is the approach used in this work.

Mesh refinement

In the model used, a smaller domain with a much more refined mesh has been created to obtain a precise solution: the mesh in this way is finer near to the centre of the sphere, where the source is placed, and the thermal gradients are strong.

Numerically this is translated in an high density of mesh elements inside the refinement volume, the small sphere: in the final mesh used the total number of elements generated is around 470'000 of which almost 370'000 in the refinement sphere, even if the volume occupied by the latter is just one thousandth of the total volume.

The following 2D image does not refer to the 3D mesh built for the simulation, but it is meant to be explicative of the general refinement procedure.

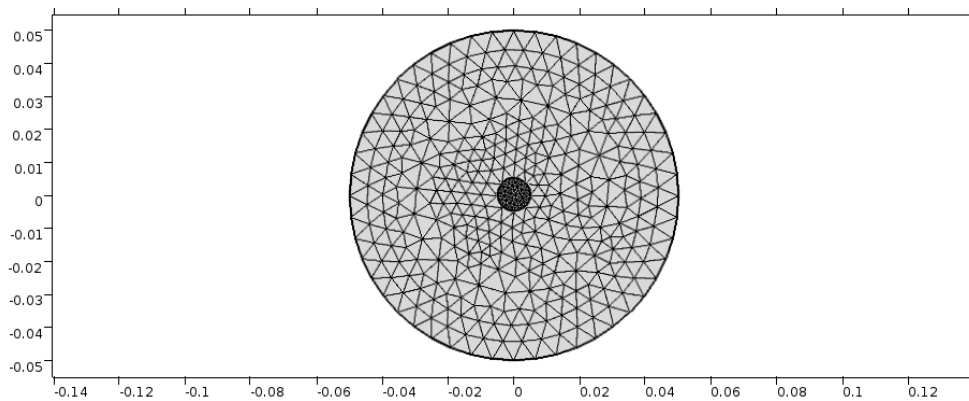


Figure 13

In the specific case of this work the strong gradients burn out in the first 2-3 mm, as the preliminary simulations determined. However, as a precautionary measure the refinement volume has been created with a 5 mm radius around the centre.

Grid independence

After computing the solution on the coarse mesh, the process of mesh refinement begins. In its simplest form, mesh refinement is the process of resolving the model with successively finer and finer meshes, comparing the results between these

different meshes. This comparison can be done by analysing the fields at one or more points in the model or by evaluating the integral of a field over some domains or boundaries, for a given time.

By comparing these scalar quantities, it is possible to judge the convergence of the solution with respect to mesh refinement. After comparing a minimum of three successive solutions, an asymptotic behaviour of the solution starts to emerge, and the changes in the solution between meshes become smaller. Eventually, these changes will be small enough that the analyst can consider the model to be converged. This is always a judgment call on the part of the analyst, who knows the uncertainties in the model inputs and the acceptable uncertainty in the results. [31]

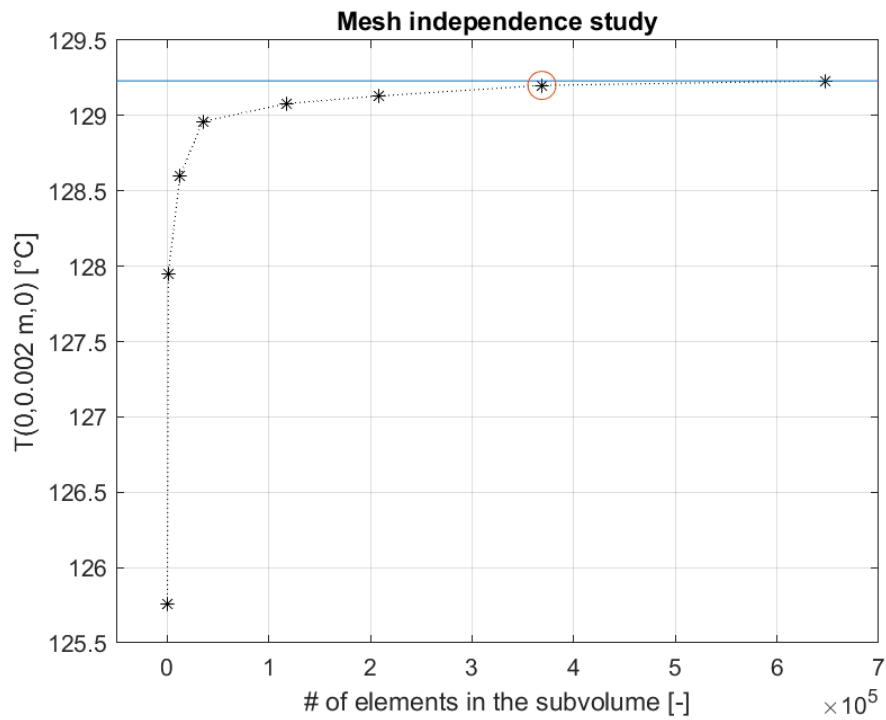


Figure 14

The mesh independence analysis highlighted a plateau in the results after the value obtained as a result of the simulation performed with 369'743 elements: it can be said that for mesh finer than that one the solution is mesh independent.

Another important aspect regarding the mesh is its quality: a mesh is said to be a good quality one when its parameters are inside certain ranges. Surely the most important parameter is the “element quality”, a parameter that keeps into account the global effectiveness of each element to compute the solution. Since it is a parameter that refers singularly to each element of the mesh the minimum value is usually taken

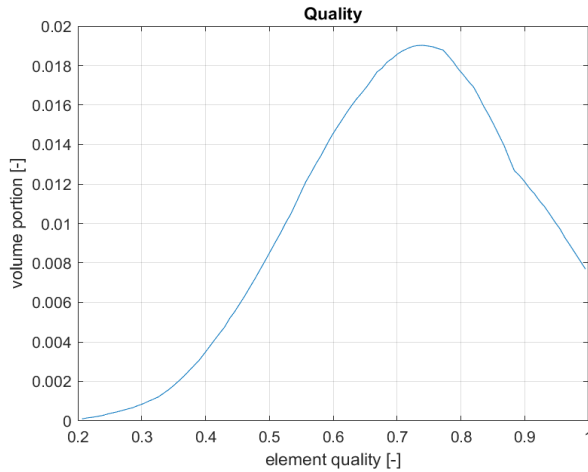


Figure 15

as a reference. As a rule of thumb the minimum element quality must be higher than 0.1. In the chosen mesh the minimum mesh quality is 0.2028 but the histogram of the element quality shows an average value well above the threshold.

Time-step independence

Alongside the mesh independence study a similar independence analysis is carried on for the timesteps.

COMSOL gives the user the possibility to choose between two different time stepping procedures:

- Adaptive, with steps adapting to the dynamic of the simulation;
- Fixed, with constant steps.

The adaptive technique allows to have smaller steps in presence of steep transients, that means significant difference in the computed values from a time step to the next one. This leads to a more efficient use of the memory and to a lower computational cost, for the same accuracy. On the other hand, given the complexity in manipulating the adaptation operation, the fixed time stepping has been preferred to perform the timestep independence analysis. At the end of this analysis the selected time step has been used as the maximum accepted value for an adaptive time stepping, to exploit the improvement in term of computational cost.

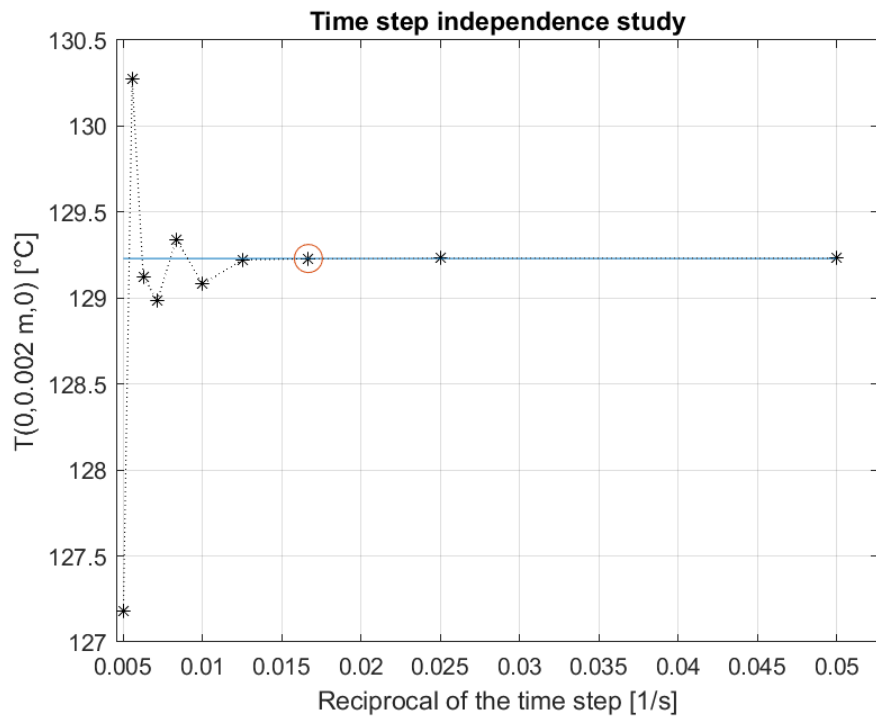


Figure 16

According to the analysis displayed in Figure 16 the maximum time step for the adaptive stepping procedure performed has been chosen to be 75 s. As it can be noticed from the convergence plot here showed some oscillations can be obtained if the time step is not small enough. This effect is even more marked at the beginning of the transient, where the residual of the solution is still considerable. Anyway, in principle, this is a problem only if the solution in this part of the transient is of interest: this has been the case during the study of the transient (parametrical analysis with respect to the time); consequently during that analysis the fixed stepping procedure has been selected, determining an additional weight in terms of computational load but making the solution acceptable with regard to independence from the size of the steps.

Parametrical analysis

The focus of the study is understanding how the area reaching a cytotoxic temperature is modulated by the changing parameters of the source and of the tissue.

Particular importance is assumed by the depth of the ablated volume with respect to the emission point. For this reason the following approach has been used:

- the cytotoxic temperature has been defined as 55°C;

- the simulations have been performed and the temperature field obtained;
- the analysis has been restricted to the y-axis of the sphere, along which the radiation is released;
- a MATLAB code has been written and run to determine the y-depth (called L) of the mentioned ablation area;
- the variable L has been plotted according to the parameter change.

In the following image, Figure 17, the segment on which the temperature data are collected is shown in red.

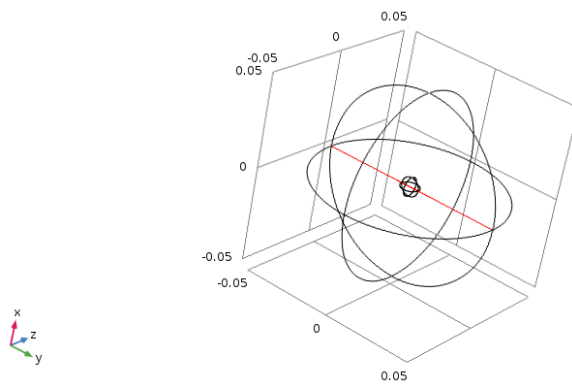


Figure 17

The shape of the temperature field along this segment is presented in the Figure 18.

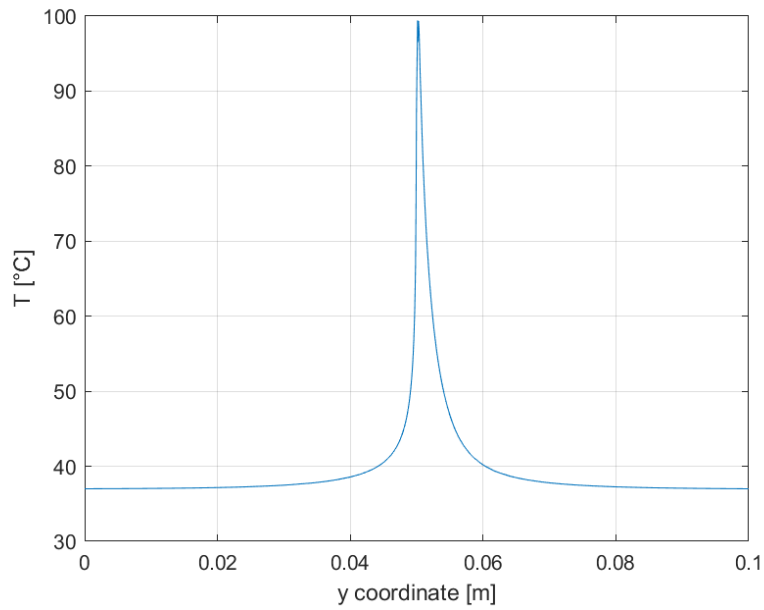


Figure 18

By determining the length L of the segment which has a temperature higher than the cytotoxic temperature an estimation of the depth of the ablation area was provided.

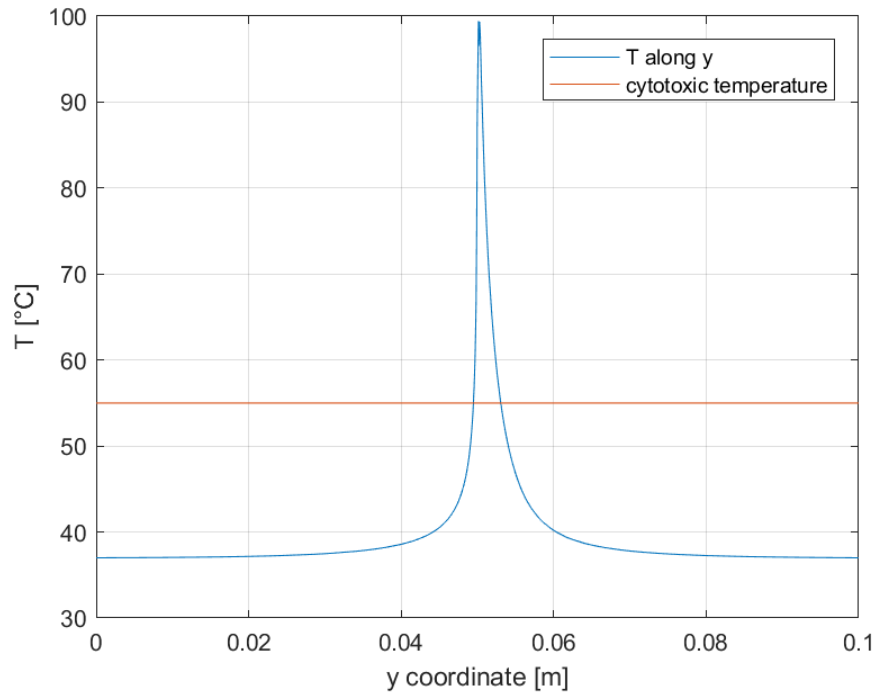


Figure 19

Inside the ablation area there are strong gradients as it is highlighted by the plot shown. The temperature increase toward the peak of the curve is very fast and this gives an idea of why it is crucial to understand how to modulate the shape, particularly in terms of penetration: a very high maximum temperature with a narrow ablation depth would be useless from the medical point of view, yet this is the typical outcome when dealing with strong absorption.

Choice of the parameters

According to the mentioned behaviour of the temperature field some of the parameters governing the evolution of the system acquire a greater relevance regarding the ablation procedure.

These are:

- the duration of the power delivery t , as the energy deposited in the body by the laser is the product between power and time. Naturally this is just a part of the overall balance that controls the temperature rise but it is expected to show some sort of direct dependence;

- the source power P , for the reason above-mentioned, that it is foreseen to bring a similar direct dependence;
- the thermal conductivity k , that can be perturbed from the reference value by inhomogeneities of various kind, rise of the body temperature or other factors.

The reference values for these parameters, around which the analysis has been performed, are:

- $t = 1000$ s;
- $P = 1$ W;
- $k = 0.52 \frac{W}{m \cdot K}$. [31]

For what concerns the imaginary part of the refractive index, and consequently the attenuation coefficient, after a preliminary study was carried out, the inadequacy of the data from the literature to describe meaningfully the temperature field during the simulation of the treatment. For this reason the absorption has been tuned to obtain a temperature field matching adequately the experiments conducted earlier at the DET.

Results

Dependence on treatment time

The treatment time can strongly vary depending on the peculiarities of the clinical condition. A standard laser ablation procedure can deposit power in the tissue for around 10-15 minutes. Anyway in the parametrical analysis it was decided to cover a larger time span, in order to clearly identify the convergence to a steady-state asymptotic situation.

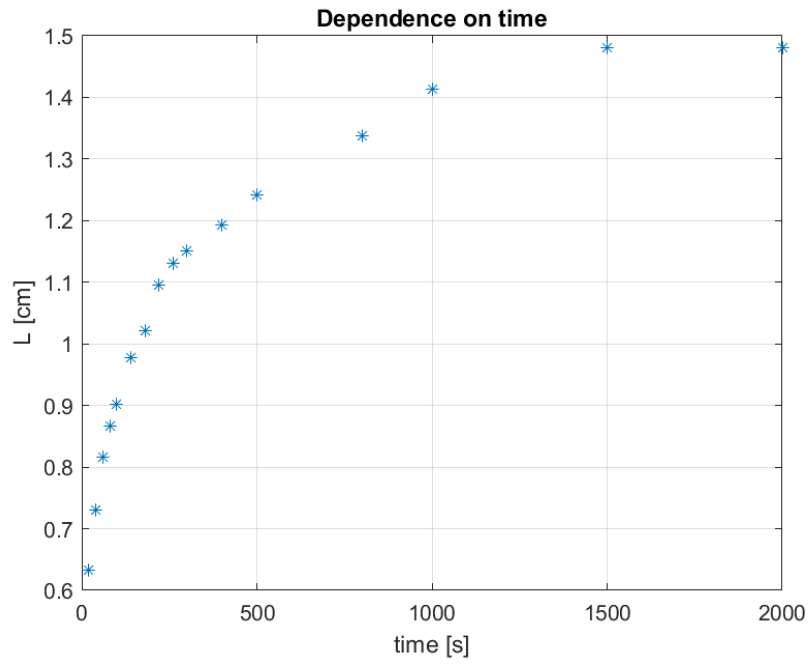


Figure 20

As expected the evolution in time of the ablation area shows a direct proportionality converging to a plateau as the steady state is approached. The search for a trend line gave as a result

$$L = 0.2 \cdot \ln(t) + 0.008$$

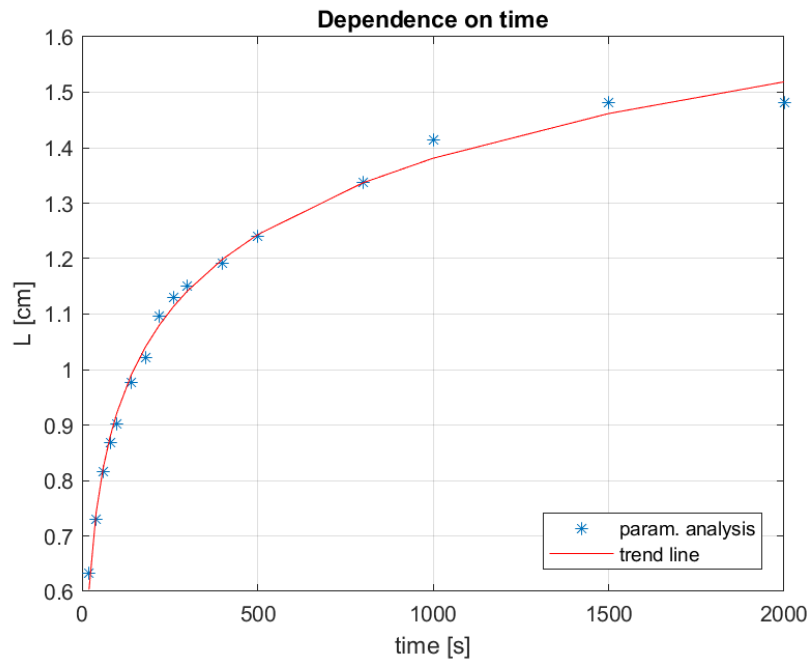


Figure 21

The trend line fits perfectly the initial transient and shows an acceptable deviation from the steady-state value, taken at 2000 s.

Dependence by the thermal conductivity

The thermal conductivity is an easily perturbed parameter: change in temperature, inhomogeneities and anisotropies can determine variation in the conductivity.

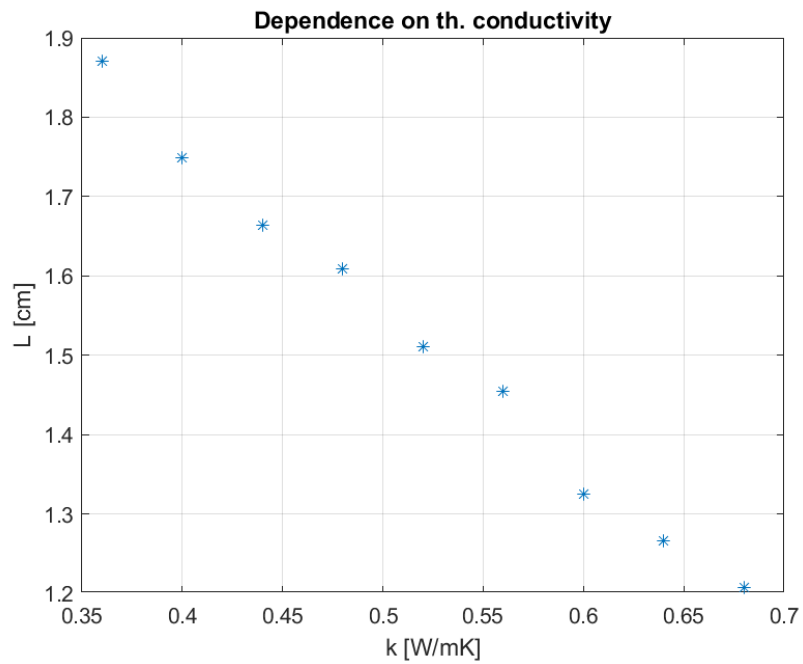


Figure 22

For this analysis the trend line is linearly decreasing. It has to be highlighted that, for each simulation, the thermal conductivity was considered constant and, for this reason, also independent from the temperature. As a matter of fact, this is an important assumption.

The equation of the trend line is:

$$L = -2.1 \cdot k + 2.6$$

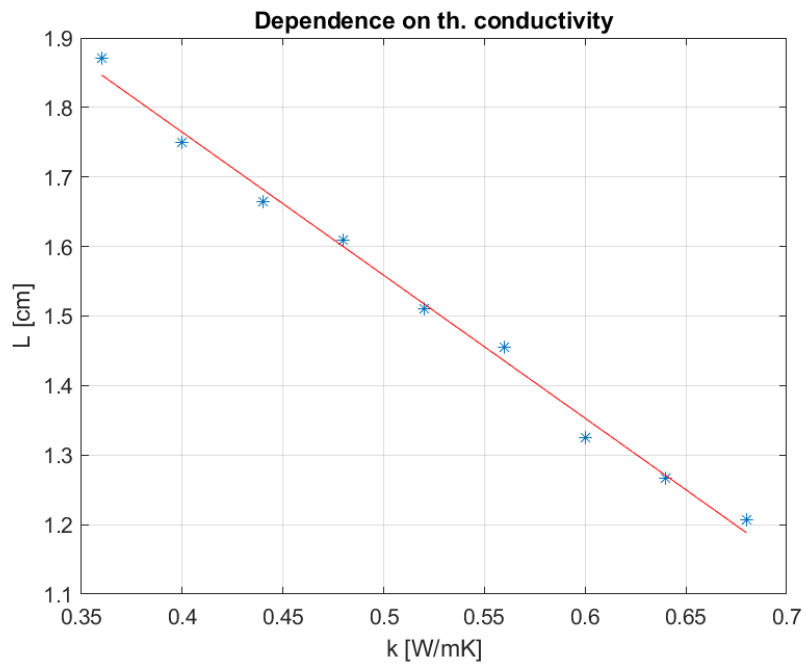


Figure 23

Dependence by the laser power

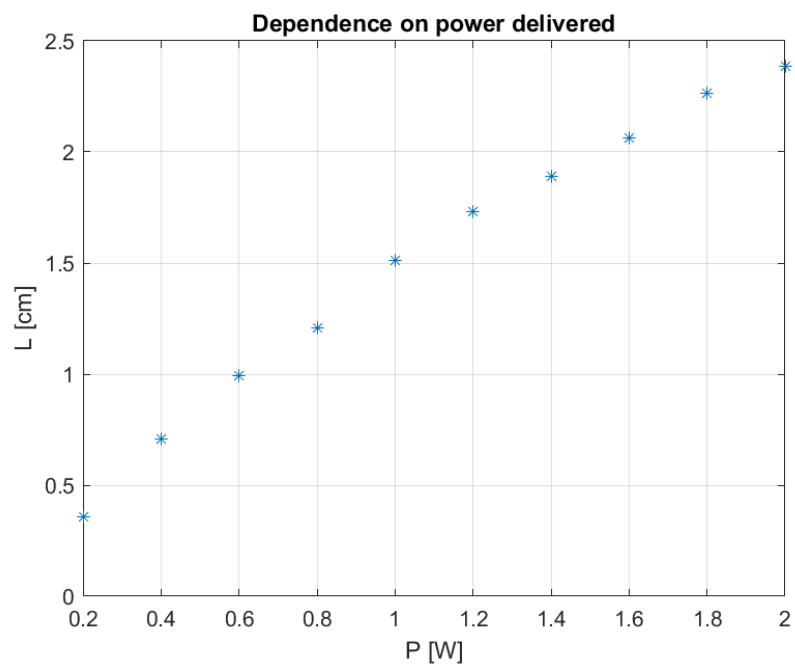


Figure 24

The dependence of the ablation depth L with respect to the power released is direct, as it was easy to foresee. The trend line is:

$$L = -0.31 \cdot P^2 + 1.8 \cdot P$$

Having forced the line to cross the origin, being meaningless an ablation depth different from zero for no power release.

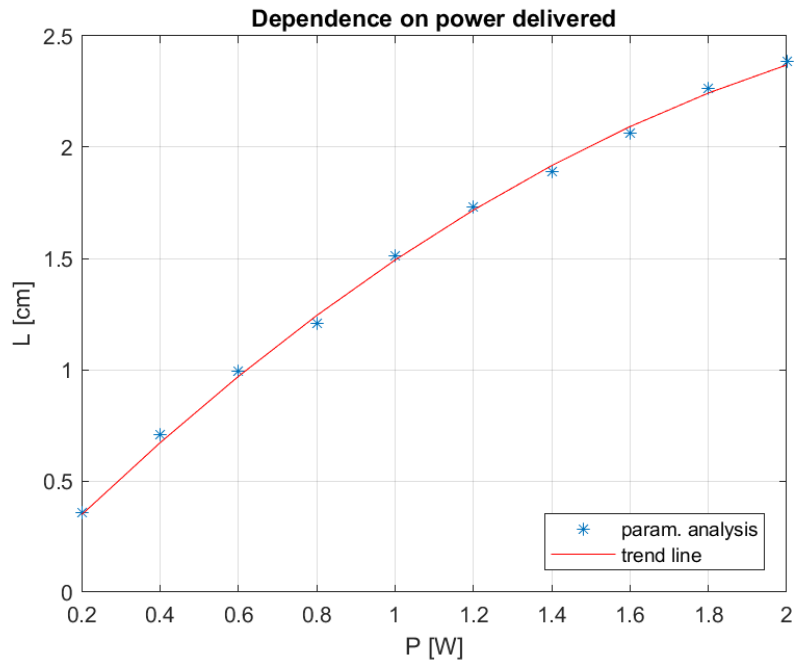


Figure 25

Experiments

The experiments have been performed in the laboratories of the Istituto Superiore Mario Boella (ISMB), inside the Polytechnic of Turin.

The aim of the experiments was to investigate the liver absorption data available from the study [28] of Giannios et al. as the results of the simulations using those values have been found incompatible with the different experiments conducted. Moreover the changes, in terms of attenuation coefficient, following an heating up of the liver samples have been analysed.

The experiments have been carried out on fresh bovine liver, which behaviour is assimilable to the human liver, even with a non-negligible discrepancy in the numerical values of the parameters involved.



Figure 26

The simple scheme shown in Fig [26] makes it easy to understand the experiment: the source emits a beam that, by passing through the sample gets attenuated. The Optical Spectrum Analyser (OSA) receive the surviving radiation, analysing its spectrum. By the comparison between the input spectrum and the output spectrum the absorption for the different wavelengths can be derived.

Experimental equipment

Source

The source employed for this experiment is a supercontinuum one, a source with a smooth spectrum, formed when a collection of nonlinear processes acts together upon a pump beam in order to cause severe spectral broadening of the original pump beam, that can be normally recognized as a peak in the spectrum. [32]

The spectrum, if analysed in air, had the shape shown in Figure 27.

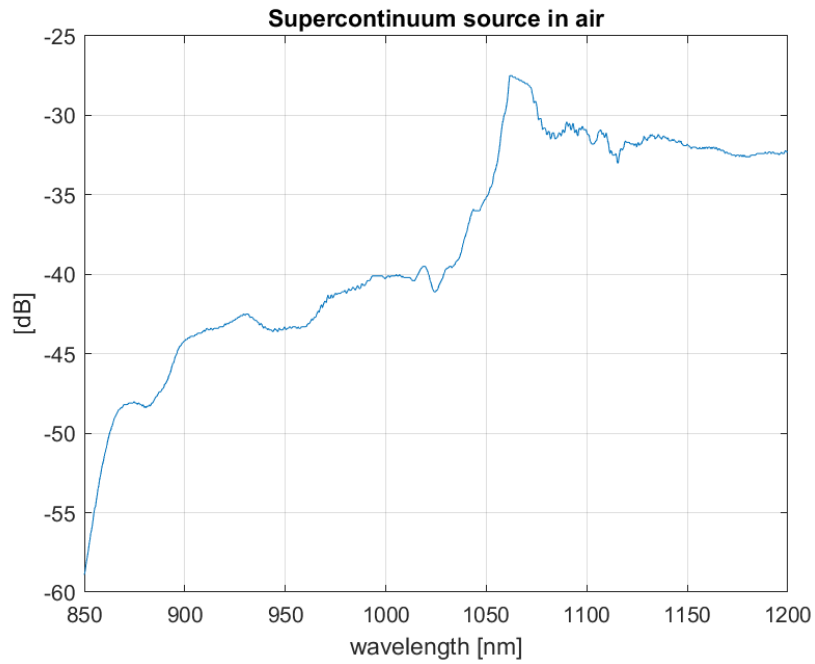


Figure 27

The reference for the results given in dB is 1 milliWatt.

The definition of the magnitude of the detected power of the beam is the following:

$$(P/P_r)_{dB} = 10 \cdot \log_{10}(P/P_r)$$

With the quantity P_r being the reference power abovementioned: 1mW.

Naturally these and all the experimental results presented in this thesis already takes into account some air attenuation that anyway occurs on a very narrow distance covered. In particular the set-up and the relative measure is displayed in Figure 28.

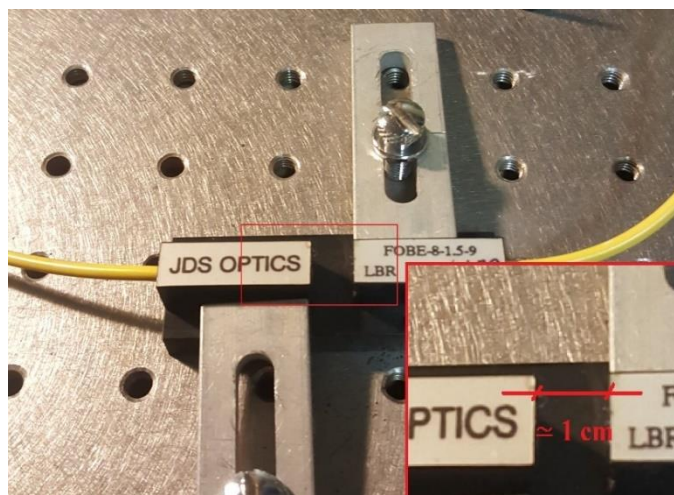


Figure 28

The distance between the tips of the emitting and the receiving fiber, in this set-up for the optical coupling, is indeed around 1 centimetre.

The generator used was a Koheras SuperK Power.



Figure 29

Transmission

The source, once emitted, was carried by an optical fiber to the superK SPLIT, a filter that allows to get rid of the spectrum for the wavelengths outside a chosen sub-area. Indeed, in principle, this could have parasitic effects.

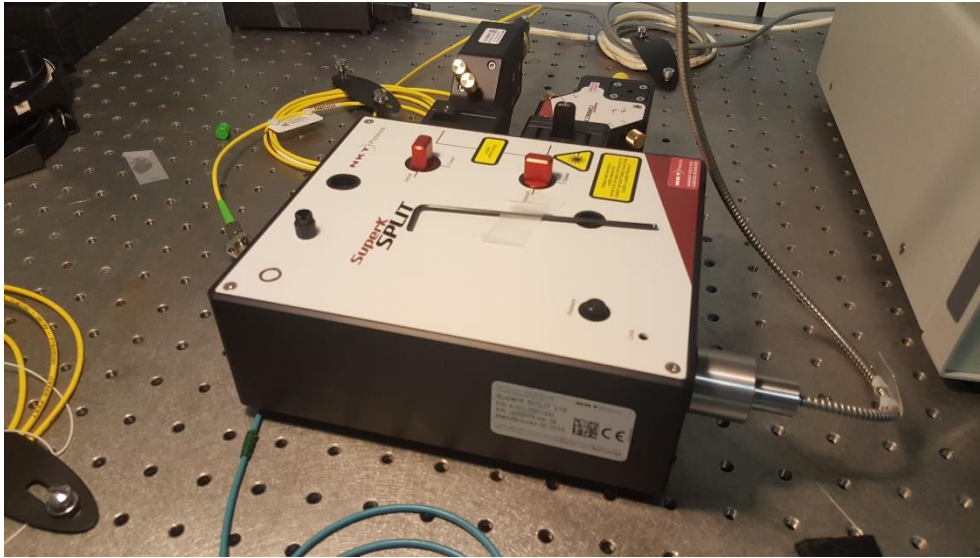


Figure 30

Then the laser radiation is brought by another fiber to the optical coupler, designed specifically for the experiment by Massimo Olivero.

The sample is put in between the emitting and the receiving fiber as displayed in the following image, Fig. [31].

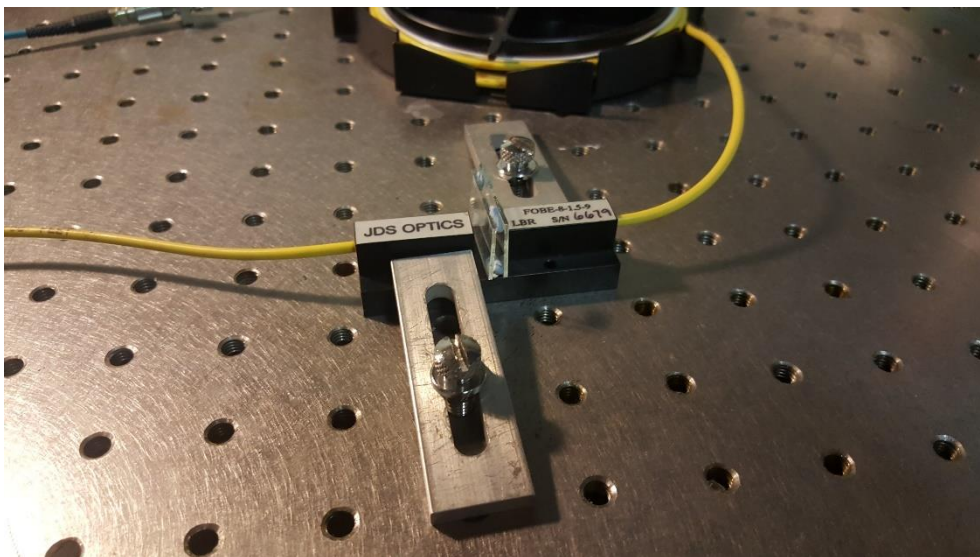


Figure 31

Naturally, the contribution of the microscopic slides to the absorption has been considered by taking as a reference the spectrum received by the fiber and analysed by the OSA, having positioned in the optical coupler the empty microscopic slides: this brought to the definition of the absorption spectrum of the slides, as the

difference between the spectrum in air and the spectrum after the transmission through the slides.

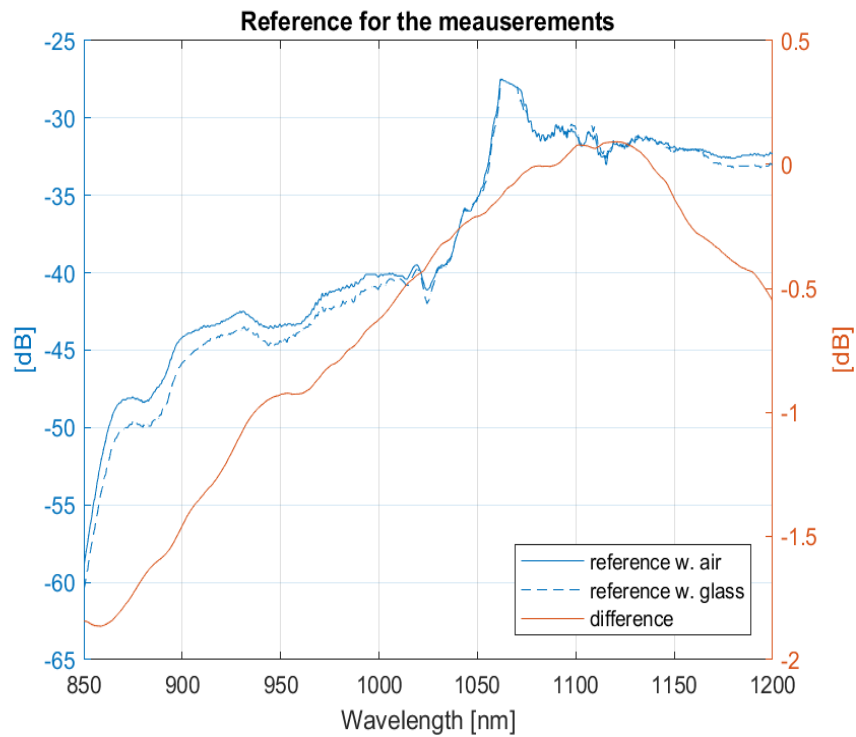


Figure 32

These preliminary measures have been conducted for a spectrum slightly narrower than the one that will be generally used later in the experiments. Anyway, as a precautionary measure, the attenuation due to the slides (red line in Fig. [32]) has been considered constant with respect to the wavelength at its maximum value, around -2 dB.

Optical Spectrum Analyser



Figure 33

The OSA is a precision instrument designed to measure and display the distribution of power of an optical source over a specified wavelength span. Its trace usually displays power in the vertical scale and the wavelength in the horizontal scale.

As far as this experiment is concerned the instrument used was the Agilent 86140: the wavelength accuracy of this instrument is 0.2 nm while the sensibility is around -70 dB. These features make the device perfectly compatible with the experimental needs.

Execution

During the first phase of the experiment the measurements were made on the fresh liver. The sample was carefully cut into small slices, with a constant effort to make the slice as homogeneous as possible. The thickness of the sample was measured and, after that, the sample was then put between microscopic slides and positioned inside the optical coupler.

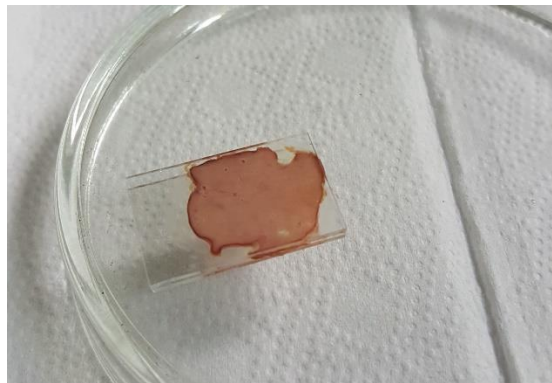


Figure 34

The set-up was then properly covered to avoid external influence on the measurement.

Having double-checked all the security measures, the source was turned on, the OSA enabled and the measurements made. The data were then made available for the post-processing.

A similar procedure has been carried out for the second phase of the experiment, after the heating up of the sample: 12 minutes in the homogeneous 75°C environment of a laboratory oven.

Results

Considerations and further assumptions

An essential preliminary consideration to the results that are here presented concerns the thickness of the samples used in the experiment: without the availability of the proper instruments (in particular a microtome) and despite the huge effort made, it was not possible to obtain a homogeneous thickness for the liver samples. This leads to the main assumption behind the results presented in this thesis: according to the measurements made the samples are assumed to be 2 mm thick.

Another important assumption when dealing with the reference spectrum was made: the microscopic slides put in the optical coupler made the air mass between the coupled fibers decrease, decreasing the air-caused absorption as well. This has been neglected.

From the point of view of the results, instead, their noisiness has been mitigated with a MATLAB function. Furthermore the results obtained for wavelengths below 900 nm were ignored, since the high variability that affected them, raising doubts on their reliability.

Data

The postprocessing of the results was made according to the following procedure.

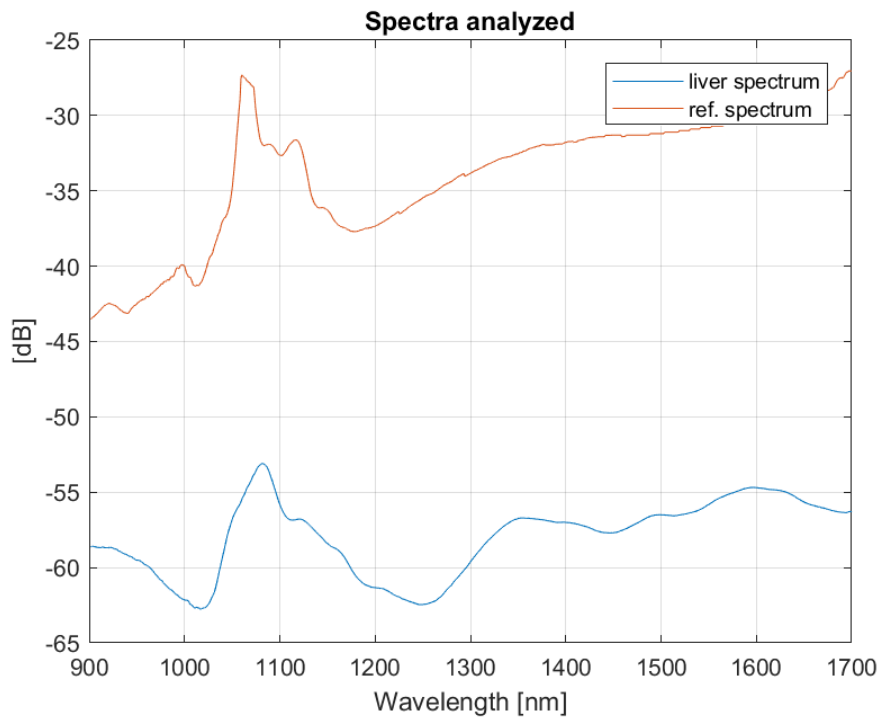


Figure 35

This is the typical result of the investigation. The spectrum of the laser radiation, after going through the sample, gets attenuated differently for every wavelength.

Applying

$$(P_{liver}/P_r)_{dB} - (P_s/P_r)_{dB} = 10 \cdot \log_{10}(P_{liver}/P_s)$$

where P_s is the source power, attenuated by the air and by the microscopic slides.

Remembering that according to the Beer-Lambert law,

$$P_{liver}/P_s = e^{-\alpha x}$$

it is easy to determine

$$\alpha = -\frac{\log(P_{liver}/P_s)}{x}$$

that means, in terms of refractive index, using the relationship already defined,

$$Im(n) = -\frac{\lambda \cdot \log(P_{liver}/P_s)}{4\pi \cdot x}$$

The first set of data tends to confirm the factor 10 discrepancy between the Giannios et al. study and the results obtained as of now.

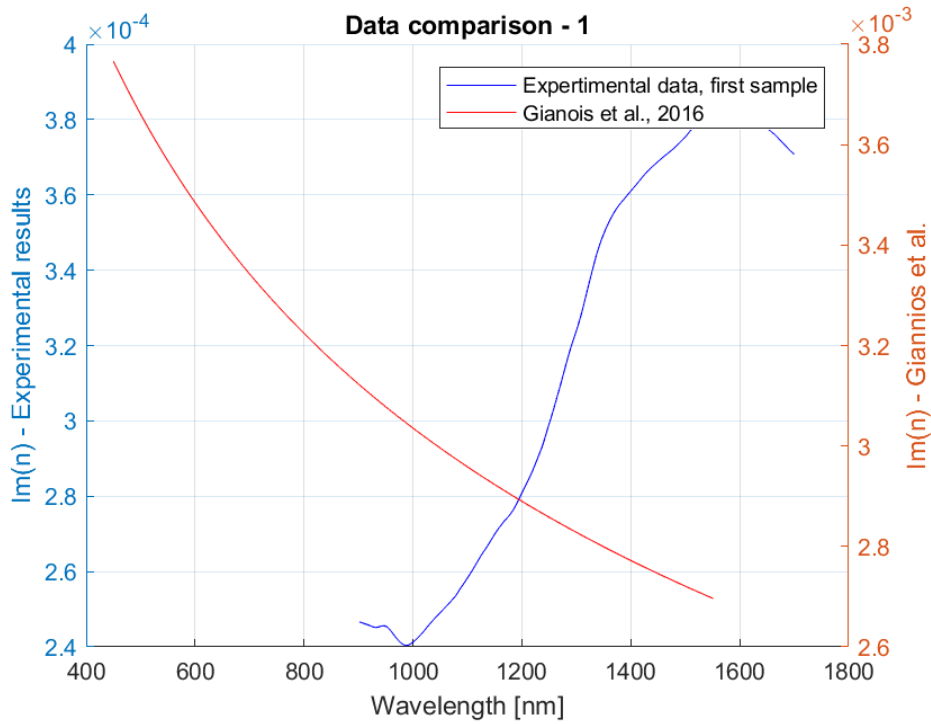


Figure 36

The dependency over the wavelength is, anyway, very different: in the span where the literature foresees an inverse dependence the extinction factor is directly increasing.

To account for the possible intrinsic variability in the procedure (for example the inclination of the microscopic slides) other measurements have been conducted on a second sample.

On the following plot it can be appreciated how, even on the same sample, the measurements underwent some major oscillation from time to time. This can be due to the inhomogeneous nature of the investigated material, to the positioning of the sample or to the optical behaviour of the set-up.

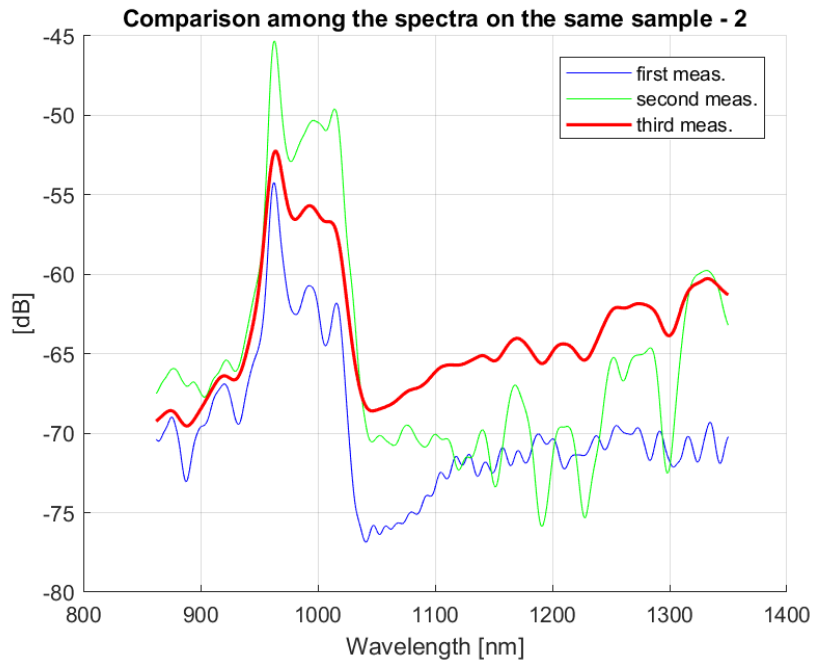


Figure 37

Since the variability, for this set of data, was definitely non-negligible, the average value was taken for the calculation of the imaginary part of the refractive index.

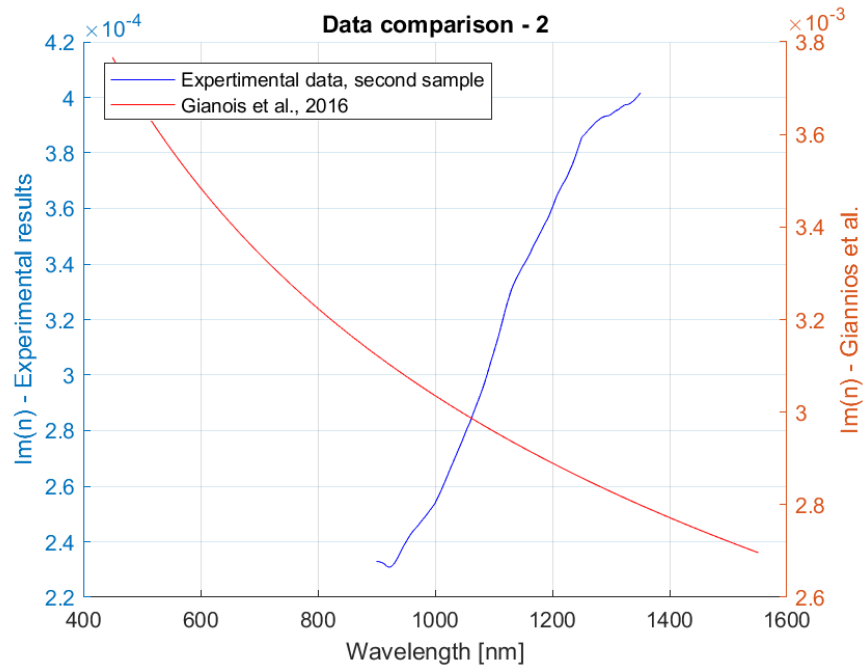
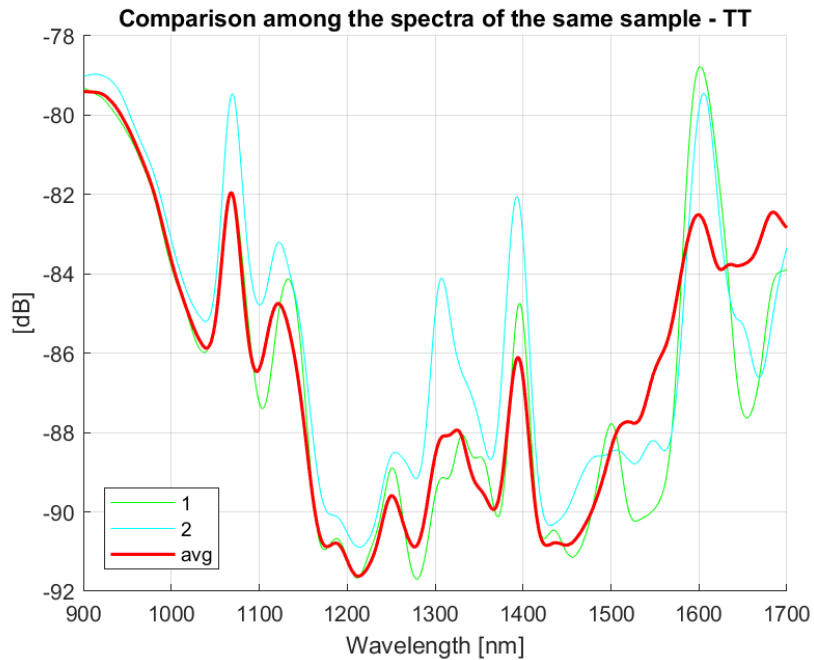


Figure 38

A similar result is obtained, confirming the first results.

In the second phase of the experiment, as mentioned in the *Procedure* section, the sample underwent a thermal treatment. In this case the results suffer a significant change.



The absorption is sharply increased and the reliability of the results is compromised, as the magnitude of the power collected by the receiving fiber is below the sensibility of the instruments. For this reason the data on the imaginary part of the refractive index get noisy. Nevertheless the behaviour, as the wavelength changes, is the same one already observed.

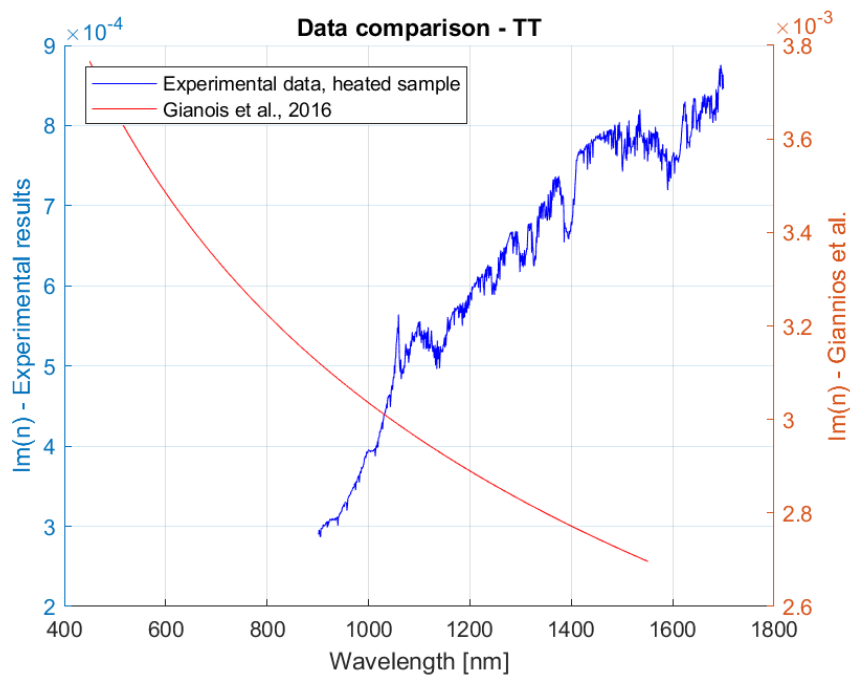


Figure 39

The values recorded, on the other hand, are pretty different. The Fig. [40] shows a comparison between the $Im(n)$ before and after the heating up, highlighting a huge increase in the absorption due to the thermal treatment.

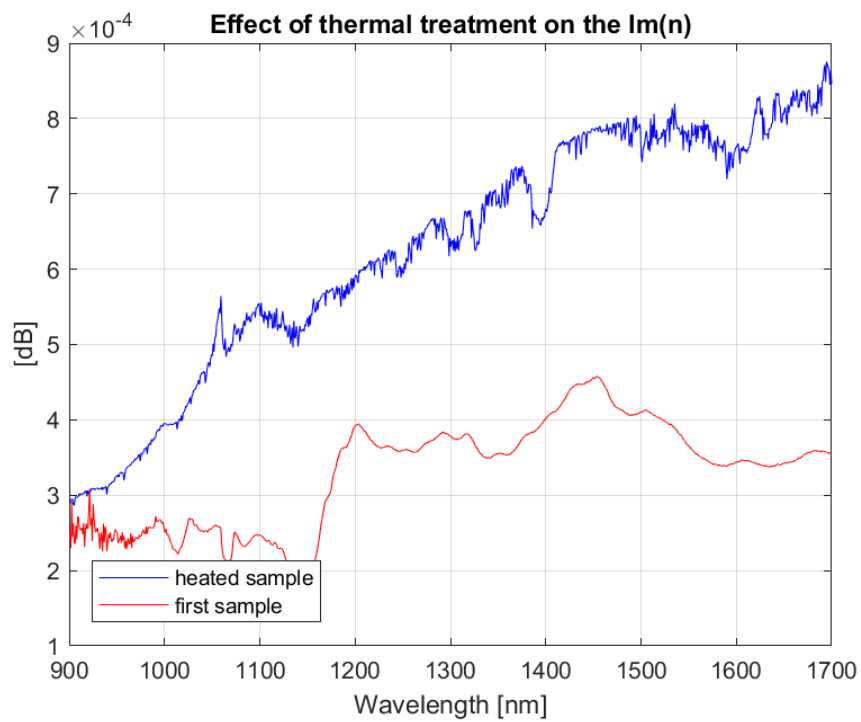


Figure 40

Conclusions

Physical understanding and experimental measurements are both essential in the rapid improvement of a technological procedure. In this thesis progresses have been achieved for both. The parametrical analysis made possible to understand the dependences of the temperature field with respect to the main parameters and highlighted the possibility to find suitable correlations to describe these.

These could be used as solid basis to investigate the influence of other phenomena present in the human body, as perfusion or metabolic heat generation, and the interdependence among parameters or their temporal evolution during the ablation procedure.

Concerning the experimental results, even if the limits of the experimental apparatus will need further investigations, the data collected during this thesis cannot be overlooked. The doubts regarding the reliability of the only source of data openly available for human liver optical absorption are now supported by experimental evidence. This will naturally have an important impact on the simulations and could possibly bring their accuracy to increase noticeably.

The tailoring of the treatment on each specific clinical case and the ability to efficiently perform and control the process is the final goal of the development, in this field. A small step in this direction has surely been made.

References

1. <https://www.who.int/en/news-room/fact-sheets/detail/cancer>, World Health Organization
2. <https://www.cancer.gov/about-cancer/understanding/what-is-cancer>, National Cancer Institute
3. Habash Riadh W.Y. et al., 2006, “Thermal therapy, part I: an introduction to thermal therapy”
4. Fiorentini G., Szasz A., 2006, “Hyperthermia today: electric energy, a new opportunity in cancer treatment”
5. Pearce J.A., 2010, “Models for thermal damage in tissues: processes and applications”
6. Dewhurst M.W., Viglianti B.L. et al., 2014., “Thermal dose requirement for tissue effect: experimental and clinical findings”
7. Carrafiello G., 2012, “Complications of microwave and radiofrequency lung ablation: Personal experience and review of the literature”
8. <https://www.comsol.com/blogs/study-radiofrequency-tissue-ablation-using-simulation/>, Frei W., COMSOL
9. <https://www.rp-photonics.com/lasers.html>, Encyclopedia of Laser Physics, RP Photonics
10. Primavesi F. et al., 2017, “Thermographic real-time-monitoring of surgical radiofrequency and microwave ablation in a perfused porcine liver model”
11. <https://www.cancer.org/cancer/liver-cancer/treating/tumor-ablation.html>, American Cancer Society
12. Escoffre J., Bouakaz A., 2016, “Therapeutic Ultrasound”
13. Keilman G.W., Kaczkowski P.J., 1998, “High-intensity focused ultrasound transducer design for surgical and hemostatic applications”
14. Knavel E.M. et al., 2013, “Tumor Ablation: Common Modalities and General Practices”
15. Tombesi et al., 2015, “Radiofrequency, microwave and laser ablation of liver tumors: time to move toward a tailored ablation technique”
16. Gough-Palmer A.L., 2008, “Laser ablation of hepatocellular carcinoma-A review”
17. Schena E., Saccomandi P., Fong Y., 2017, “Laser Ablation for Cancer: Past, Present and Future”

18. Abramczyk, H., 2005, "Introduction to Laser Spectroscopy"
19. Pogliano, J., 2017, "Analysis of fiber probes for tumor laser ablation"
20. <http://hyperphysics.phy-astr.gsu.edu/hbase/phyopt/totint.html#c1>, Georgia State University
21. <http://hyperphysics.phy-astr.gsu.edu/hbase/optmod/fibopt.html>, Georgia State University
22. Bruggmoser G., 2012, "Some aspects of quality management in deep regional hyperthermia"
23. <https://www.fbgs.com/technology/fbg-principle/>, FBGS
24. Polito D. et al., 2015, "A needle-like probe for temperature monitoring during laser ablation based on FBG: Manufacturing and characterization"
25. Cappelli S. et al., 2015, "Magnetic Resonance-compatible needle-like probe based on Bragg grating technology for measuring temperature during Laser Ablation"
26. Schena E. et al., 2013, "Monitoring of temperature increase and tissue vaporization during laser interstitial thermotherapy of ex vivo swine liver by computed tomography"
27. Grand View Research, Inc., 2018, "Tumor Ablation Market Size, Share & Trends Analysis Report By Treatment, By Application, By Technology And Segment Forecasts"
28. Giannios er al, 2016, "Visible to near-infrared refractive properties of freshly-excised human-liver tissues: marking hepatic malignancies"
29. <https://www.comsol.com/multiphysics/mesh-refinement>, COMSOL
30. User Guide, COMSOL v5.2a
31. <https://itis.swiss/virtual-population/tissue-properties/database/thermal-conductivity/>, IT IS
32. <https://www.nktphotonics.com/lasers-fibers/product/superk-split-spectral-supercontinuum-splitter/>, NKT